

Uncertainty Propagation of Correlated Quaternion and Euclidean States Using the Gauss-Bingham Density

JACOB E. DARLING
KYLE J. DEMARS

A new probability density function, called the Gauss-Bingham density, is proposed and studied in the context of uncertainty propagation. The Gauss-Bingham density quantifies the correlation between a quaternion and Euclidean states on the cylindrical manifold on which these states naturally exist. The Gauss-Bingham density, including its canonical form, is developed. In order to approximate the temporal evolution of the uncertainty, an unscented transform for the Gauss-Bingham density is first developed. The sigma points are then transformed according to given (potentially) nonlinear system dynamics, and the maximum weighted log-likelihood parameters of the Gauss-Bingham density are recovered. Uncertainty propagation using the Gauss-Bingham density does not rely on a small angle assumption to project the uncertainty in the quaternion into a three parameter representation as does the predictor of the multiplicative extended Kalman filter, so its accuracy does not suffer when propagating large attitude uncertainties. Two simulations are presented to show the process and efficacy of uncertainty propagation using the Gauss-Bingham density and to compare it to the multiplicative extended Kalman filter.

Manuscript received March 23, 2016; released for publication March 29, 2016.

Refereeing of this contribution was handled by Igor Gilitschenski.

Authors' addresses: Department of Mechanical and Aerospace Engineering, Missouri University of Science and Technology, Rolla, MO, 65409 USA. (E-mail: {jed7w2,demarsk}@mst.edu).

1557-6418/16/\$17.00 © 2016 JAIF

I. INTRODUCTION

Consider the planar translation and rotation of a body, which are quantified by Cartesian position coordinates and heading angle, respectively. The position of the body is typically assumed Gaussian-distributed since it is not bounded to a given interval; however, the heading angle cannot be assumed Gaussian-distributed since it is required to be in the interval $[-\pi, \pi)$ and the support of the Gaussian density is infinite. A circular density, such as the wrapped normal density or von Mises density, which are defined on the interval $[-\pi, \pi)$, can be used to quantify the heading angle. The position and heading angle of the body are correlated in general, but they are properly quantified by two different densities; they must, therefore, be quantified under a common state density in order to properly represent their correlation.

Estimation approaches have been developed when the state consists of *only* a von Mises- or wrapped normal-distributed circular variable [1], [2]. The predictor step of these approaches, which propagates the state uncertainty in time, calculates or approximates the temporal evolution of the von Mises or wrapped normal density; however, they do not extend to a state with *both* a circular variable and other Euclidean (additive and unbounded) variables. Mardia and Sutton first proposed a state density to quantify a circular and Euclidean variable in which the state density is constructed as the product of a von Mises density and a Gaussian density conditioned on the von Mises-distributed variable [3]. The Gauss von Mises density is constructed in a similar manner to quantify a state with both a circular variable and other Euclidean variables as the product of a multivariate Gaussian density and von Mises density conditioned on the multivariate Gaussian-distributed variable [4].

A single circular variable can be used to quantify the heading angle, or one-dimensional attitude, of a body. Now consider the case when the three-dimensional attitude and other Euclidean states (such as position, velocity, angular velocity, etc.) of a body are quantified by an attitude quaternion and Cartesian coordinates, respectively. The attitude quaternion exists on the unit hypersphere and is antipodally symmetric; that is, opposing quaternions represent the same attitude. The attitude quaternion is a globally nonsingular attitude representation, and thus, it is a popular choice to represent the three-dimensional attitude of a body [5]–[7].

The Bingham density can be used to quantify the uncertainty of an attitude quaternion on the unit hypersphere [8], [9]. The Bingham density is a zero-mean Gaussian density conditioned on the unit hypersphere and is antipodally symmetric, so it is a proper probabilistic representation of the attitude quaternion because antipodal quaternions represent the same physical attitude and, therefore, must be equiprobable. Estimation approaches have been developed for a state that consists

only of an attitude quaternion [10]–[12]. In particular, [12] leverages an unscented transform to propagate the uncertainty of the Bingham-distributed attitude quaternion when the system dynamics are nonlinear. These approaches, however, do not quantify the correlation between the Bingham-distributed attitude quaternion and other Euclidean variables.

A state density that is similar to the Bingham density has been proposed to quantify the dual quaternion representing the pose (position and attitude) of a body [13]; however, this density does not extend to arbitrarily high dimensions to include the velocity, angular velocity, and other Euclidean states since it is constructed using a dual quaternion. The partially wrapped normal density has recently been proposed, which wraps m coordinates of an n -dimensional Gaussian density in order to quantify the correlation between m angular and $n - m$ Euclidean states [14]. This density applies to arbitrarily high m and n , so it can potentially be used to represent the uncertainty of a rotation sequence representing the three-dimensional attitude and other Euclidean states of a body. Because the temporal evolution of a rotation sequence is potentially singular [5]–[7], the temporal evolution of this uncertainty representation will be potentially singular as well.

In order to avoid this potential singularity, this work proposes a new state density, called the Gauss-Bingham density, which can be used to represent the uncertainty of an attitude quaternion and other Euclidean states of a body. The Gauss-Bingham density, which is born as the product of a Gaussian density and a Bingham density that is conditioned on the Gaussian-distributed random variable, quantifies the correlation between an antipodally symmetric s -dimensional unit vector and an r -dimensional vector of Euclidean states on their natural manifold, the unit hypercylinder. To approximate the temporal evolution of the Gauss-Bingham density given (potentially) nonlinear system dynamics, an unscented transformation [15]–[17] is developed for the Gauss-Bingham density. The sigma points generated by the unscented transform are transformed according to the nonlinear system dynamics, and the maximum weighted log-likelihood parameters of the Gauss-Bingham density are recovered from the sigma points. Uncertainty propagation using the Gauss-Bingham density is developed for arbitrary dimensions r and s , and s can then be specialized to $s = 1$ or $s = 3$ to represent the one- and three-dimensional attitude quaternion, respectively.

In order to present the uncertainty propagation of a Gauss-Bingham-distributed state vector, first a review of the attitude representations used is presented in Section II. A review of the Gaussian and Bingham densities is then presented in Section III. The Gauss-Bingham density, including the correlation structure between the Gaussian and conditional Bingham densities, is developed in Section IV. Uncertainty propagation of a Gauss-Bingham-distributed state vector is presented in Section V, which includes the unscented transform and

maximum weighted log-likelihood parameter estimation for the Gauss-Bingham density. Two simulations of uncertainty propagation using the Gauss-Bingham density are presented in Section VI. The first simulation propagates the uncertainty of the one-dimensional attitude quaternion and angular velocity of a body undergoing torque-free motion where the Gauss-Bingham density can easily be visualized in order to provide an intuitive example of this uncertainty propagation method. The second simulation propagates the uncertainty of the three-dimensional relative position, relative velocity, attitude quaternion, and angular velocity of a chase spacecraft with respect to a target spacecraft. A Monte Carlo approach and the predictor of the multiplicative extended Kalman filter are also simulated in order to evaluate the efficacy of uncertainty propagation using the Gauss-Bingham density and to compare it to more conventional methods.

II. ATTITUDE REPRESENTATIONS, KINEMATICS, AND DYNAMICS

Many different representations can be used to parameterize the attitude of a body. The following subsections provide a brief overview of the attitude representations, quaternion kinematics, and angular velocity dynamics used in the subsequent sections; [5]–[7] provide a comprehensive overview of these topics. The attitude matrix, which is a nine-parameter attitude representation, is used to fundamentally quantify the attitude of a body. In practice, the attitude matrix is difficult to quantify directly since it possesses six constraints, so a three or four parameter attitude representation is typically used to parameterize the attitude matrix in order to overcome this difficulty. Three parameter attitude representations provide a one-to-one representation; however, they are potentially singular. To avoid this singularity, a four parameter attitude representation, which is globally nonsingular, is typically used. Four parameter attitude representations are constrained in some way, since three parameters are sufficient to define attitude. Four parameter attitude representations also provide a two-to-one representation of attitude; that is, two sets of the same four parameter representation quantify the same physical attitude.

A. Attitude Matrix

The attitude of a body is fundamentally quantified by the attitude matrix, \mathbf{A} . The attitude matrix is defined as the orientation matrix that rotates the expression of a vector in the “ I ” coordinate-frame to its expression in the “ B ” coordinate-frame. This orientation matrix is denoted by T_I^B and is defined according to

$$\mathbf{x}^B = T_I^B \mathbf{x}^I \triangleq \mathbf{A} \mathbf{x}^I,$$

where \mathbf{x}^I and \mathbf{x}^B denote the physical vector $\mathbf{x} \in \mathbb{R}^3$ expressed in the I and B frames, respectively, and \mathbb{R}^n

represents n -dimensional Euclidean space. Typically, the I frame is taken to be an inertially-fixed frame and the B frame is taken to be a body-fixed frame of interest, but it is not required that the I frame be inertially fixed for these attitude representations to be valid.

Orientation matrices exist in the n -dimensional special orthogonal group, which is given by $SO(n) \triangleq \{T \in \mathbb{R}^{n \times n} : T^T T = I = T T^T, \det T = 1\}$, where $\det \cdot$ represents the determinant operator. Because orientation matrices are in $SO(n)$, they satisfy the following properties:

$$T_I^B = T_C^B T_I^C \quad \text{and} \quad T_B^I = [T_I^B]^{-1} = [T_I^B]^T. \quad (1)$$

These properties allow the rotation matrix relating a reference frame to the body frame, and thus quantifying the attitude error between these frames, to be expressed as

$$\delta A \triangleq T_R^B = T_I^B T_R^I = T_I^B [T_I^R]^T = A \hat{A}^T, \quad (2)$$

where the “ R ” coordinate frame represents the reference frame and \hat{A} represents the attitude matrix of the reference frame. As the attitude error approaches zero, $A \rightarrow \hat{A}$ and $\delta A \rightarrow I$, where I represents the identity matrix of appropriate dimension.

B. Axis-Angle

An intuitive four parameter representation of a rotation in three dimensions is the axis-angle representation. Euler’s theorem states that any rotation in three dimensions can be accomplished by a single rotation. The axis of this rotation is known as the Euler axis and is quantified by the unit vector \mathbf{e} . Define the corresponding angle of rotation about the Euler axis to be $\theta \in [-\pi, \pi)$. The axis-angle representation of this rotation is then given by the parameter set $\{\mathbf{e}, \theta\}$. If the sign of *both* the Euler axis *and* the rotation angle are changed, the rotation defined by the axis-angle representation is unaffected and the two-to-one representation of attitude using the axis-angle representation is apparent. The attitude matrix is given in terms of the Euler axis and rotation angle about the Euler axis by

$$A = I - \sin\theta[\mathbf{e} \times] + (1 - \cos\theta)[\mathbf{e} \times]^2, \quad (3)$$

where $[\mathbf{a} \times]$ represents the skew-symmetric cross product matrix of the arbitrary vector $\mathbf{a} \in \mathbb{R}^3$ and $[\mathbf{e} \times]^2 \triangleq [\mathbf{e} \times][\mathbf{e} \times]$.

C. Rotation Vector

A three parameter representation of a rotation in three dimensions is born as the product of the Euler axis and the rotation angle about the Euler axis as

$$\boldsymbol{\theta} = \theta \mathbf{e}. \quad (4)$$

This attitude parameterization is known as the rotation vector. The rotation vector is a one-to-one representation of attitude, which is apparent since $\{\mathbf{e}, \theta\}$ and $\{-\mathbf{e}, -\theta\}$, which quantify the same rotation, result in

the same rotation vector. The rotation vector is singular due to the potential discontinuity that can occur when propagating the rotation vector. The norm of the rotation vector is constrained to be no greater than π since $\theta \in [-\pi, \pi)$. During propagation, if the magnitude of the rotation vector is equal to π and has a positive temporal derivative, then the rotation vector must instantaneously change sign since $\{\mathbf{e}, \pm\pi\}$ and $\{-\mathbf{e}, \pm\pi\}$ represent equivalent rotations.

The axis-angle representation can be found from the rotation vector according to

$$\mathbf{e} = \frac{\boldsymbol{\theta}}{\|\boldsymbol{\theta}\|} \quad \text{and} \quad \theta = \|\boldsymbol{\theta}\|. \quad (5)$$

It is apparent from (5) that the Euler axis is undefined if the rotation angle is zero. This is not an issue, however, since this corresponds to a rotation angle of zero and $A = I$ in this case. The attitude matrix in terms of the rotation vector is given by substituting (3) into (5) to give the attitude matrix as

$$A = I - \sin\|\boldsymbol{\theta}\| \left[\frac{\boldsymbol{\theta}}{\|\boldsymbol{\theta}\|} \times \right] + (1 - \cos\|\boldsymbol{\theta}\|) \left[\frac{\boldsymbol{\theta}}{\|\boldsymbol{\theta}\|} \times \right]^2. \quad (6)$$

D. Attitude Quaternion

The attitude quaternion is a four parameter attitude representation and is defined by

$$\bar{\mathbf{q}} = \begin{bmatrix} \mathbf{q} \\ q \end{bmatrix} \in \mathbb{S}^3,$$

where $\mathbf{q} \triangleq [q_x \ q_y \ q_z]^T$ and q are the vector and scalar parts of the quaternion, respectively, and $\mathbb{S}^s \triangleq \{\mathbf{z} \in \mathbb{R}^{s+1} : \mathbf{z}^T \mathbf{z} = 1\}$ represents the s -dimensional unit hypersphere. Two important quaternion operations are multiplication and inversion, which are given for unit quaternions by

$$\bar{\mathbf{q}} \otimes \bar{\mathbf{r}} = \begin{bmatrix} r\mathbf{q} + q\mathbf{r} - \mathbf{q} \times \mathbf{r} \\ qr - \mathbf{q} \cdot \mathbf{r} \end{bmatrix} \quad \text{and} \quad \bar{\mathbf{q}}^{-1} = \begin{bmatrix} -\mathbf{q} \\ q \end{bmatrix},$$

where $\bar{\mathbf{q}} \otimes \bar{\mathbf{r}}$ represents the quaternion product of $\bar{\mathbf{q}}$ and $\bar{\mathbf{r}}$ and $\bar{\mathbf{q}}^{-1}$ represents the inverse of $\bar{\mathbf{q}}$. The quaternion multiplication is defined in this way such that successive rotations can be represented by multiplying quaternions in the same order as rotation matrices. Quaternion multiplication is not commutative, i.e. $\bar{\mathbf{q}} \otimes \bar{\mathbf{r}} \neq \bar{\mathbf{r}} \otimes \bar{\mathbf{q}}$ in general.

The attitude quaternion is the most widely used attitude representation because it is not singular and quaternion multiplication and inversion are used to represent sequential and opposite rotations. Equivalent properties as those given for orientation matrices in (1) can be expressed using quaternions according to

$$\bar{\mathbf{q}}_I^B = \bar{\mathbf{q}}_C^B \otimes \bar{\mathbf{q}}_I^C \quad \text{and} \quad \bar{\mathbf{q}}_B^I = [\bar{\mathbf{q}}_I^B]^{-1}.$$

The identity quaternion is defined as $\bar{\mathbf{p}} \triangleq [\mathbf{0}^T \ 1]^T$ and is the quaternion representing zero rotation, such that

$$\bar{\mathbf{q}} = \bar{\mathbf{q}} \otimes \bar{\mathbf{p}} = \bar{\mathbf{p}} \otimes \bar{\mathbf{q}} \quad \text{and} \quad \bar{\mathbf{p}} = \bar{\mathbf{q}} \otimes \bar{\mathbf{q}}^{-1} = \bar{\mathbf{q}}^{-1} \otimes \bar{\mathbf{q}}.$$

Using these relationships, the attitude error given in (2) can be expressed using quaternions according to

$$\delta\bar{\mathbf{q}} = \bar{\mathbf{q}} \otimes \hat{\mathbf{q}}^{-1},$$

where $\delta\bar{\mathbf{q}}$ is the quaternion representation of $\delta\mathbf{A}$ and $\hat{\mathbf{q}}$ is the reference quaternion. As the attitude error approaches zero, $\bar{\mathbf{q}} \rightarrow \hat{\mathbf{q}}$ and $\delta\bar{\mathbf{q}} \rightarrow \bar{\mathbf{p}}$.

The attitude quaternion is related to the axis-angle attitude representation and rotation vector according to

$$\bar{\mathbf{q}} = \begin{bmatrix} \mathbf{e} \sin \frac{\theta}{2} \\ \cos \frac{\theta}{2} \end{bmatrix} = \begin{bmatrix} \frac{\boldsymbol{\theta}}{\|\boldsymbol{\theta}\|} \sin \frac{\|\boldsymbol{\theta}\|}{2} \\ \cos \frac{\|\boldsymbol{\theta}\|}{2} \end{bmatrix}. \quad (7)$$

The unit-norm constraint imposed on the attitude quaternion is apparent in (7) due to trigonometric identities. It is also apparent in (7) that the attitude quaternion is a two-to-one and antipodal attitude parameterization since $\{\mathbf{e}, \theta\}$ and $\{-\mathbf{e}, -\theta\}$, and therefore $\bar{\mathbf{q}}$ and $-\bar{\mathbf{q}}$, represent equivalent rotations. Equation (7) is solved for the axis-angle attitude representation given the attitude quaternion according to

$$\theta = 2 \arccos q \quad \text{and} \quad \mathbf{e} = (1 - q^2)^{-1/2} \mathbf{q}.$$

After finding the axis-angle attitude representation, (4) can be used to find the equivalent rotation vector attitude representation according to

$$\boldsymbol{\theta} = \frac{2 \arccos q}{(1 - q^2)^{1/2}} \mathbf{q}. \quad (8)$$

E. Quaternion Kinematics and Attitude Dynamics

If $\bar{\mathbf{q}}$ is used to represent the equivalent rotation as the attitude matrix, \mathbf{A} , the temporal evolution of the attitude quaternion is given by

$$\dot{\bar{\mathbf{q}}} = \frac{1}{2} \begin{bmatrix} \boldsymbol{\omega} \\ 0 \end{bmatrix} \otimes \bar{\mathbf{q}}, \quad (9)$$

where $\boldsymbol{\omega}$ is angular velocity of the B frame with respect to the I frame expressed in the B frame. This is a kinematic relationship defining the temporal evolution of the attitude quaternion given the angular velocity of the body and is the rotational equivalent of the kinematic relationship between translational position and velocity.

If I is taken to be an inertial frame, the temporal evolution of the angular velocity for a rigid body is given by

$$\mathbf{J}^B \dot{\boldsymbol{\omega}} = \boldsymbol{\tau}^B - \boldsymbol{\omega} \times \mathbf{J}^B \boldsymbol{\omega}, \quad (10)$$

where \mathbf{J}^B is the inertia tensor of the body and $\boldsymbol{\tau}^B$ is the external torque acting on the body, both expressed in the B frame. This is the dynamic relationship relating the temporal evolution of the angular velocity to the inertia tensor of the body and the net external torque acting on the body. This relationship is the rotational analog to the dynamic relationship relating the temporal evolution of the translational velocity to the mass and net external force acting on the body.

III. PROBABILITY DENSITY FUNCTIONS

Before constructing the Gauss-Bingham density, the Gaussian and Bingham densities, which are used to construct the Gauss-Bingham density, are first presented in this section. Furthermore, some of their useful properties, including the applicability of probabilistically representing the attitude quaternion with the Bingham density, are presented.

A. Gaussian Density

The Gaussian density is given for a random vector $\mathbf{x} \in \mathbb{R}^r$ by

$$p_g(\mathbf{x}; \mathbf{m}, \mathbf{P}) = |\mathbf{P}|^{-1/2} \exp\{-\frac{1}{2}(\mathbf{x} - \mathbf{m})^T \mathbf{P}^{-1}(\mathbf{x} - \mathbf{m})\}, \quad (11)$$

where $\mathbf{m} \in \mathbb{R}^r$ is the mean and $\mathbf{P} = \mathbf{P}^T > \mathbf{0} \in \mathbb{R}^{r \times r}$ is the covariance of the Gaussian density.

B. Canonical Gaussian Density

The standard normal density, which is denoted as the canonical Gaussian density for consistent nomenclature with the canonical form of other densities, is introduced by substituting the transformation

$$\mathbf{x} = \mathbf{S}\mathbf{z} + \mathbf{m} \quad \text{where} \quad \mathbf{P} = \mathbf{S}\mathbf{S}^T \quad (12)$$

into (11), which yields the canonical Gaussian density as

$$\tilde{p}_g(\mathbf{z}) = p_g(\mathbf{z}; \mathbf{0}, \mathbf{I}) = (2\pi)^{-r/2} \exp\{-\frac{1}{2}\mathbf{z}^T \mathbf{z}\},$$

where the tilde notation is used to denote the canonical form of the density.

C. Bingham Density

The Bingham density is an antipodally symmetric density on the unit hypersphere that is a zero-mean Gaussian density conditioned on the unit hypersphere. Because antipodal attitude quaternions ($\bar{\mathbf{q}}$ and $-\bar{\mathbf{q}}$) represent the same attitude, the Bingham density rigorously quantifies the uncertainty in the quaternion representation of attitude without ambiguity between $\bar{\mathbf{q}}$ and $-\bar{\mathbf{q}}$. The Bingham density is defined for a random unit vector $\bar{\mathbf{q}} \in \mathbb{S}^s$ and is given by [8], [9]

$$p_b(\bar{\mathbf{q}}; \mathbf{M}, \mathbf{Z}) = F^{-1}(\mathbf{Z}) \exp\{\bar{\mathbf{q}}^T \mathbf{M} \mathbf{Z} \mathbf{M}^T \bar{\mathbf{q}}\}, \quad (13)$$

where $\mathbf{M} \in \text{SO}(s+1)$ is the orientation matrix describing the orientation of the density on the unit hypersphere, $\mathbf{Z} \in \mathbb{R}^{(s+1) \times (s+1)}$ is a diagonal matrix of concentration parameters with nondecreasing diagonal elements $Z_1 \leq \dots \leq Z_s \leq Z_{s+1} \stackrel{\Delta}{=} 0$, and $F(\mathbf{Z})$ is the normalization constant that ensures that $p_b(\bar{\mathbf{q}}; \mathbf{M}, \mathbf{Z})$ is a valid probability density function. The Bingham density possesses the property that $p_b(\bar{\mathbf{q}}; \mathbf{M}, \mathbf{Z}) = p_b(\bar{\mathbf{q}}; \mathbf{M}, \mathbf{Z} + c\mathbf{I})$ for all $c \in \mathbb{R}$; thus, Z_{s+1} can be defined to be zero with an appropriate choice of c for a given Bingham density without any change to the characteristics of the density.

An abuse of notation is used for $\bar{\mathbf{q}}$ because it is used to represent both a generic antipodally symmetric unit vector of arbitrary dimension s as well as the attitude quaternion; when $\bar{\mathbf{q}} \in \mathbb{S}^1$ or $\bar{\mathbf{q}} \in \mathbb{S}^3$, $\bar{\mathbf{q}}$ is a valid attitude quaternion representing the one- and three-dimensional orientation of a body, respectively. Whether $\bar{\mathbf{q}}$ represents a generic antipodally symmetric unit vector or the attitude quaternion is clear in the surrounding context.

The parameters of \mathbf{Z} control how tightly clustered the Bingham density is around its mean direction, while the orientation matrix, \mathbf{M} , specifies the mean direction itself. The normalization constant of the Bingham density is given by the hypergeometric function of a matrix argument according to

$$\begin{aligned} F(\mathbf{Z}) &= \int_{\mathbb{S}^s} \exp\{\bar{\mathbf{q}}^T \mathbf{Z} \bar{\mathbf{q}}\} d\mathbb{S}^s \\ &= |\mathbb{S}^s| {}_1F_1\left(\frac{1}{2}; \frac{s+1}{2}; \mathbf{Z}\right), \end{aligned} \quad (14)$$

where $|\mathbb{S}^s|$ represents the area of the unit hypersphere \mathbb{S}^s and ${}_1F_1(\cdot; \cdot; \cdot)$ represents the hypergeometric function of a matrix argument. The normalization constant is independent of the orientation matrix, which is intuitive since the orientation matrix simply changes the orientation of the density on the unit hypersphere. Many methods exist for calculating the normalization constant, including series expansions [18], saddle point approximations [19], [20], the holonomic gradient method [21], and interpolation of precomputed tabulated values [22]. In this work, the integral in (14) is numerically integrated directly in order to obtain the normalizing constant of the Bingham density.

Parallels between the parameters of the well-known and well-understood Gaussian density and the parameters of the Bingham density can be drawn in order to better understand the Bingham density. The Bingham density is a directional density; that is, it probabilistically quantifies the direction of a unit vector in \mathbb{S}^s . The orientation matrix, \mathbf{M} , is similar to the mean of the Gaussian density, \mathbf{m} , in that it specifies the mean *direction* of the Bingham density, while \mathbf{m} specifies the mean *location* of the Gaussian density. The matrix of concentration parameters of the Bingham density, \mathbf{Z} , is similar to the covariance matrix of the Gaussian density, \mathbf{P} , in that it specifies how tightly clustered the Bingham density is about its mean direction. Making the elements of \mathbf{Z} more negative leads to a more tightly clustered density about the mean direction for the Bingham density similarly to how decreasing \mathbf{P} leads to a more tightly clustered density about the mean for the Gaussian density. It is important to note that \mathbf{Z} is not the covariance of the Bingham density; however, they are directly related, as discussed in Section III-E.

Representing the uncertainty of an attitude quaternion using the Bingham density has three key advantages as compared to other methods of attitude uncertainty representation:

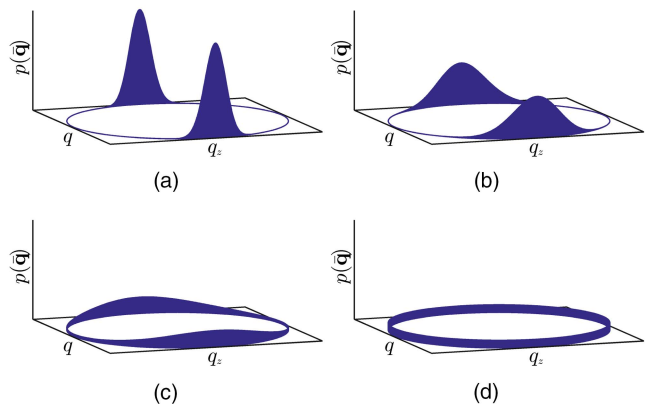


Fig. 1. Bingham densities on \mathbb{S}^1 for $\mathbf{M} = \mathbf{I}$ and varying values of Z_1 . (a) $Z_1 = -50$. (b) $Z_1 = -10$. (c) $Z_1 = -2$. (d) $Z_1 = 0$.

- The Bingham density is antipodally symmetric; thus, antipodal quaternions $\bar{\mathbf{q}}$ and $-\bar{\mathbf{q}}$ (which represent the same physical attitude) are equiprobable,
- the Bingham density quantifies the uncertainty of the attitude quaternion $\bar{\mathbf{q}}$ on its natural manifold \mathbb{S}^3 instead of projecting the attitude uncertainty into a local tangent space, which can potentially incur approximation errors, and
- the Bingham density possesses a simple representation of a uniformly distributed attitude quaternion on this manifold when the \mathbf{Z} matrix is null.

In order to visualize how the Bingham density represents the distribution of an attitude quaternion, the Bingham density is illustrated in \mathbb{S}^1 and \mathbb{S}^2 , where straightforward visualizations exist. The Bingham density is first shown for one-dimensional attitude uncertainty quantification, where the axis of rotation is defined to be the z -axis. In this case, the attitude quaternion simplifies to

$$\bar{\mathbf{q}} = \begin{bmatrix} 0 \\ 0 \\ q_z \\ q \end{bmatrix} = \begin{bmatrix} 0 \\ 0 \\ \sin(\theta/2) \\ \cos(\theta/2) \end{bmatrix} \in \mathbb{S}^1, \quad (15)$$

where θ is the magnitude of the rotation about the z -axis. Fig. 1 shows the Bingham-distributed one-dimensional attitude quaternion for the identity orientation matrix and different values of Z_1 . Observation of Fig. 1 shows that the Bingham density is antipodally symmetric; that is, $\bar{\mathbf{q}}$ and $-\bar{\mathbf{q}}$ are equiprobable. Further observation highlights that as Z_1 becomes more negative, the uncertainty in the attitude quaternion decreases. Similarly, as Z_1 approaches zero, the uncertainty in the attitude quaternion increases until $Z_1 = 0$, in which case the attitude quaternion is uniformly-distributed.

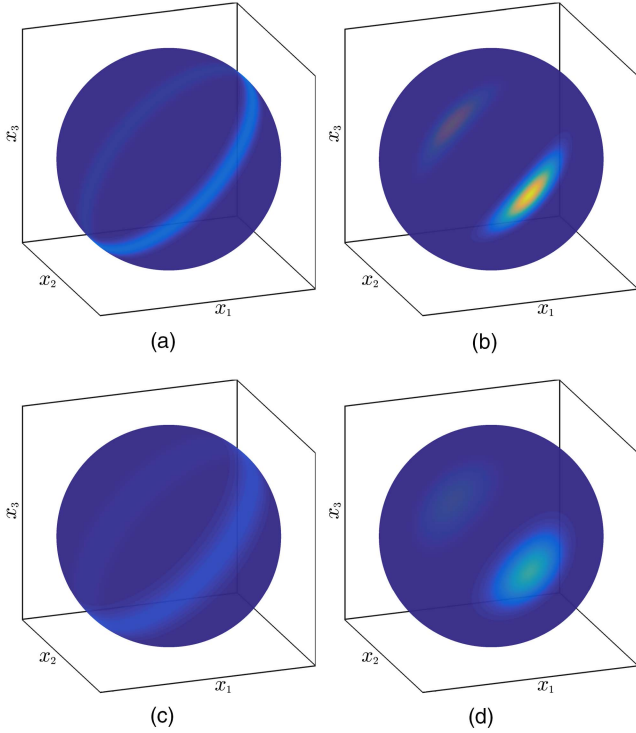


Fig. 2. Bingham densities on \mathbb{S}^2 for varying values of Z_1 and Z_2 . (a) $Z_1 = -100, Z_2 = 0$. (b) $Z_1 = -100, Z_2 = -10$. (c) $Z_1 = -25, Z_2 = 0$. (d) $Z_1 = -25, Z_2 = -10$.

No valid attitude quaternion exists on \mathbb{S}^2 ; however, the Bingham density for the unit vector $\bar{\mathbf{q}} = [x_1 \ x_2 \ x_3]^T \in \mathbb{S}^2$ is illustrated in Fig. 2 for the orientation matrix

$$\mathbf{M} = \begin{bmatrix} \frac{\sqrt{2}}{2} & \frac{\sqrt{2}}{2} & 0 \\ 0 & 0 & 1 \\ \frac{\sqrt{2}}{2} & -\frac{\sqrt{2}}{2} & 0 \end{bmatrix}$$

and varying values of Z_1 and Z_2 to demonstrate how the \mathbf{Z} matrix affects the Bingham density in this dimension. When $Z_1 = Z_2 = 0$, all $\bar{\mathbf{q}}$ are equiprobable. When Z_2 is zero, the $\bar{\mathbf{q}}$ along a great circle defined by the orientation matrix \mathbf{M} are equiprobable, as observed in Figs. 2(a) and 2(c). In this case, the Z_1 parameter dictates how tightly clustered the probability density of $\bar{\mathbf{q}}$ is along the great circle. When Z_2 decreases from zero, the probability density of $\bar{\mathbf{q}}$ increases in the direction defined by the orientation matrix \mathbf{M} , as observed in Figs. 2(b) and 2(d).

No straightforward visualization of the Bingham density exists in \mathbb{S}^3 . Similar trends, however, are present as the entries of \mathbf{Z} change for the Bingham densities in \mathbb{S}^3 as they do for the Bingham density in \mathbb{S}^1 and \mathbb{S}^2 . A uniformly distributed attitude quaternion is given by the null \mathbf{Z} matrix, and as Z_1, Z_2 , and Z_3 decrease, the uncertainty in the attitude quaternion decreases. If any of the Z_1, Z_2 , and Z_3 are equal to zero, then the attitude quaternion becomes equiprobable around a

higher-dimensional circle or sphere, similar to Figs. 2(a) and 2(c) for the Bingham density in \mathbb{S}^2 .

D. Canonical Bingham Density

The canonical Bingham density is introduced by substituting the transformation

$$\bar{\mathbf{q}} = \mathbf{M}\bar{\mathbf{p}} \quad (16)$$

into (13), which yields the canonical Bingham density as

$$\tilde{p}_b(\bar{\mathbf{p}}; \mathbf{Z}) = p_b(\bar{\mathbf{p}}; \mathbf{I}, \mathbf{Z}) = F^{-1}(\mathbf{Z}) \exp\{\bar{\mathbf{p}}^T \mathbf{Z} \bar{\mathbf{p}}\}.$$

The canonical Bingham density still depends on the matrix of concentration parameters, \mathbf{Z} ; however, the elements of $\bar{\mathbf{p}}$ are uncorrelated.

While the canonical Bingham density is only defined on \mathbb{S}^s , it is still possible to express its mean and covariance in \mathbb{R}^{s+1} . First, define the expected value operator as

$$E_p\{f(\mathbf{x})\} = \int_{\Omega} f(\mathbf{x})p(\mathbf{x})d\mathbf{x},$$

where Ω represents the support of the probability density function $p(\mathbf{x})$ and $f(\mathbf{x})$ is an arbitrary (potentially) nonlinear function defined on Ω . Due to the antipodal symmetry of the canonical Bingham density, its mean in \mathbb{R}^{s+1} is

$$E_{\tilde{p}_b}\{\bar{\mathbf{p}}\} = \mathbf{0}.$$

Because the elements of $\bar{\mathbf{p}}$ are uncorrelated, the covariance of the canonical Bingham density in \mathbb{R}^{s+1} is given by (2.9) from [8] as

$$E_{\tilde{p}_b}\{\bar{\mathbf{p}}\bar{\mathbf{p}}^T\} = \text{diag}[f_1 \ f_2 \ \cdots \ f_{s+1}], \quad (17)$$

where the $\text{diag} \mathbf{v}$ operator constructs a matrix with diagonal entries defined by the arbitrary row vector \mathbf{v} and

$$f_i \triangleq F^{-1}(\mathbf{Z}) \frac{\partial F(\mathbf{Z})}{\partial Z_i}.$$

The f_i terms satisfy several important properties, given by

$$\sum_{i=1}^{s+1} f_i = 1 \quad (18a)$$

$$f_i > 0, \quad i = 1, 2, \dots, s+1 \quad (18b)$$

$$\lim_{Z_i \rightarrow -\infty} f_i = 0^+, \quad i = 1, 2, \dots, s \quad (18c)$$

$$\lim_{Z_1, Z_2, \dots, Z_s \rightarrow -\infty} f_{s+1} = 1^-. \quad (18d)$$

These properties will be exploited when determining the weights of sigma points of the unscented transform for the canonical Gauss-Bingham density in Section V-B. In order to obtain the $\partial F(\mathbf{Z})/\partial Z_i$ necessary to calculate the f_i , (14) is differentiated with respect to each Z_i , and the resulting integral expressions are evaluated numerically.

E. Mean and Covariance of the Bingham Density

Like the canonical Bingham density, the mean of the Bingham density is given in \mathbb{R}^{s+1} as

$$E_{p_b} \{\bar{\mathbf{q}}\} = \mathbf{0}$$

due to antipodal symmetry. The covariance of the Bingham density in \mathbb{R}^{s+1} is defined by $E_{p_b} \{\bar{\mathbf{q}}\bar{\mathbf{q}}^T\}$. In order to calculate this expected value, its argument is first pre- and post-multiplied by $\mathbf{M}\mathbf{M}^T = \mathbf{I}$, such that the covariance can be expressed as

$$E_{p_b} \{\bar{\mathbf{q}}\bar{\mathbf{q}}^T\} = E_{p_b} \{\mathbf{M}\mathbf{M}^T \bar{\mathbf{q}}\bar{\mathbf{q}}^T \mathbf{M}\mathbf{M}^T\}. \quad (19)$$

Introducing the transformation of variables defined in (16) and noting that \mathbf{M} is deterministic, (19) can be expressed as

$$E_{p_b} \{\bar{\mathbf{q}}\bar{\mathbf{q}}^T\} = \mathbf{M} E_{\tilde{p}_b} \{\bar{\mathbf{p}}\bar{\mathbf{p}}^T\} \mathbf{M}^T. \quad (20)$$

$E_{\tilde{p}_b} \{\bar{\mathbf{p}}\bar{\mathbf{p}}^T\}$ is simply the covariance of the canonical Bingham density, which is defined by (17). Substituting (17) into (20) yields the covariance of the Bingham density in \mathbb{R}^{s+1} as

$$E_{p_b} \{\bar{\mathbf{q}}\bar{\mathbf{q}}^T\} = \mathbf{M} \text{diag}[f_1 \quad f_2 \cdots f_{s+1}] \mathbf{M}^T,$$

which is seen to be a similarity transformation of the covariance of the canonical Bingham density according to the orientation matrix of the Bingham density.

IV. GAUSS-BINGHAM DENSITY

The Gauss-Bingham density quantifies a state vector composed of a Gaussian-distributed vector, $\mathbf{x} \in \mathbb{R}^r$, and a Bingham-distributed unit vector, $\bar{\mathbf{q}} \in \mathbb{S}^s$, on its natural manifold defined by $\mathbb{R}^r \times \mathbb{S}^s$. Before constructing the Gauss-Bingham density, first consider the motivating example of manipulating two jointly Gaussian-distributed random vectors given by \mathbf{x} and \mathbf{y} into the product of the density of \mathbf{x} and the density of \mathbf{y} conditioned on \mathbf{x} . The joint density of $[\mathbf{x}^T \ \mathbf{y}^T]^T$ is Gaussian and is given by

$$p_g \left(\begin{bmatrix} \mathbf{x} \\ \mathbf{y} \end{bmatrix}; \begin{bmatrix} \mathbf{m}_x \\ \mathbf{m}_y \end{bmatrix}, \begin{bmatrix} \mathbf{P}_x & \mathbf{P}_{xy} \\ \mathbf{P}_{xy}^T & \mathbf{P}_y \end{bmatrix} \right),$$

where \mathbf{m} and \mathbf{P} represent the mean and covariance of their subscripted vector(s), respectively. The density of \mathbf{y} conditioned on \mathbf{x} is Gaussian-distributed and is given by [23]

$$\begin{aligned} p_g(\mathbf{y} | \mathbf{x}; \mathbf{m}_{y|x}(\mathbf{x}), \mathbf{P}_{y|x}) \\ = p_g(\mathbf{y} | \mathbf{x}; \mathbf{m}_y + \mathbf{P}_{xy}^T \mathbf{P}_x^{-1} (\mathbf{x} - \mathbf{m}_x), \mathbf{P}_y - \mathbf{P}_{xy}^T \mathbf{P}_x^{-1} \mathbf{P}_{xy}), \end{aligned}$$

where $\mathbf{m}_{y|x}(\mathbf{x})$ and $\mathbf{P}_{y|x}$ are the mean and covariance, respectively, of \mathbf{y} conditioned on \mathbf{x} . It is interesting to note the functional dependence of $\mathbf{m}_{y|x}$ on \mathbf{x} . From the definition of conditional probability, it follows that the

joint density of \mathbf{x} and \mathbf{y} can be expressed as

$$\begin{aligned} p_g \left(\begin{bmatrix} \mathbf{x} \\ \mathbf{y} \end{bmatrix}; \begin{bmatrix} \mathbf{m}_x \\ \mathbf{m}_y \end{bmatrix}, \begin{bmatrix} \mathbf{P}_x & \mathbf{P}_{xy} \\ \mathbf{P}_{xy}^T & \mathbf{P}_y \end{bmatrix} \right) = p_g(\mathbf{x}; \mathbf{m}_x, \mathbf{P}_x) \\ \times p_g(\mathbf{y} | \mathbf{x}; \mathbf{m}_y + \mathbf{P}_{xy}^T \mathbf{P}_x^{-1} (\mathbf{x} - \mathbf{m}_x), \mathbf{P}_y - \mathbf{P}_{xy}^T \mathbf{P}_x^{-1} \mathbf{P}_{xy}). \quad (21) \end{aligned}$$

The conditional mean and covariance of $p(\mathbf{y} | \mathbf{x})$ are not restricted to be

$$\mathbf{m}_{y|x}(\mathbf{x}) = \mathbf{m}_y + \mathbf{P}_{xy}^T \mathbf{P}_x^{-1} (\mathbf{x} - \mathbf{m}_x) \quad (22a)$$

$$\mathbf{P}_{y|x} = \mathbf{P}_y - \mathbf{P}_{xy}^T \mathbf{P}_x^{-1} \mathbf{P}_{xy} \quad (22b)$$

for the definition of conditional probability to be valid; however, (22) must hold for the result to be Gaussian-distributed.

The left- and right-hand sides of (21) express the joint Gaussian density of $[\mathbf{x}^T \ \mathbf{y}^T]^T$ in two different forms. In the case where the vectors \mathbf{x} and \mathbf{y} are jointly Gaussian-distributed, as they are in this example, little if anything is gained by manipulating the left-hand side of (21) into the right-hand side of (21); however, in the case when one or both of the jointly distributed vectors are not Gaussian-distributed, correlation between the vectors can be introduced in a similar fashion to (21) by utilizing the definition of conditional probability. This allows the density of two jointly distributed random vectors, \mathbf{x}_1 and \mathbf{x}_2 , to be written as the product of the density of \mathbf{x}_1 and the density of \mathbf{x}_2 conditioned on \mathbf{x}_1 ; i.e.

$$p(\mathbf{x}_1, \mathbf{x}_2) = p(\mathbf{x}_1) p(\mathbf{x}_2 | \mathbf{x}_1).$$

Using the definition of conditional probability, the Gauss-Bingham density is constructed as the product of a Gaussian density and a Bingham density conditioned on the Gaussian-distributed random variable as

$$p_{gb}(\mathbf{x}; \mathbf{m}, \mathbf{P}, \mathbf{M}(\mathbf{z}), \mathbf{Z}) \triangleq p_g(\mathbf{x}; \mathbf{m}, \mathbf{P}) p_b(\bar{\mathbf{q}}; \mathbf{M}(\mathbf{z}), \mathbf{Z}), \quad (23)$$

where $\mathbf{x} = [\mathbf{x}^T \ \bar{\mathbf{q}}^T]^T$. The Bingham density is conditioned on the Gaussian-distributed random variable \mathbf{x} through the orientation matrix $\mathbf{M}(\mathbf{z})$ using the transformation of variables that defines the canonical Gaussian density, which is given by (12). The orientation matrix is expressed using \mathbf{z} (the random variable corresponding to the canonical Gaussian density) instead of \mathbf{x} for better numerical stability since \mathbf{z} is nondimensional. The functional dependence of the orientation matrix on \mathbf{z} is discussed in Section IV-A.

The Gauss-Bingham density possesses the following favorable properties for probabilistically quantifying the attitude quaternion (when $s = 1$ or $s = 3$) and other Euclidean states:

- The Gauss-Bingham density is antipodally symmetric in the attitude quaternion; thus, antipodal quaternions $\bar{\mathbf{q}}$ and $-\bar{\mathbf{q}}$ (which represent the same physical attitude) are equiprobable,

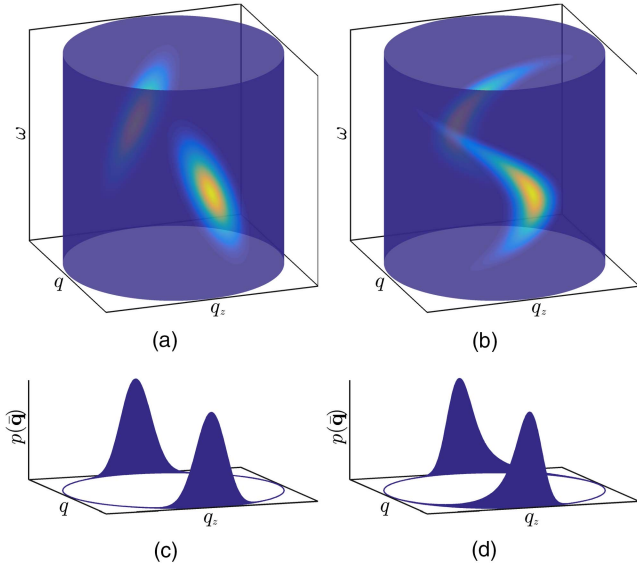


Fig. 3. Gauss-Bingham densities on $\mathbb{R}^1 \times \mathbb{S}^1$ for a linear and quadratic correlation structure. (a) Linear correlation. (b) Quadratic correlation. (c) Marginalized quaternion. (d) Marginalized quaternion.

- the Gauss-Bingham density quantifies the uncertainty of Euclidean states and the attitude quaternion on their natural manifold $\mathbb{R}^r \times \mathbb{S}^s$, and
- the Gauss-Bingham density possesses a simple representation of an equiprobable attitude quaternion for a given angular velocity when the \mathbf{Z} matrix is null.

In order to illustrate these properties, consider an application of the Gauss-Bingham density to quantify the uncertainty of the one-dimensional attitude quaternion and angular velocity of a body undergoing rotation about the z -axis. In this case, the state vector is defined as

$$\mathbf{x} = \begin{bmatrix} \omega \in \mathbb{R}^1 \\ \bar{\mathbf{q}} \in \mathbb{S}^1 \end{bmatrix} \in \mathbb{R}^1 \times \mathbb{S}^1, \quad (24)$$

where ω is the angular velocity about the z -axis and $\bar{\mathbf{q}}$ is the one-dimensional attitude quaternion of the body, which is defined by (15). No correlation structure for the orientation matrix, $\mathbf{M}(\mathbf{z})$, has yet been defined. Before formally defining this correlation structure, first consider two types of correlation, which are introduced into a set of parameters used to specify $\mathbf{M}(\mathbf{z})$: linear and quadratic. Figs. 3(a) and 3(b) show examples of the Gauss-Bingham density (with $Z_1 \neq 0$) for the linear and quadratic correlation structures, respectively. The marginalized attitude quaternion for the linear and quadratic correlation structures are shown in Figs. 3(c) and 3(d), respectively. It can be observed in these figures that the probability of the antipodal attitude quaternions is equal for any given angular velocity, which is a desirable property as these quaternions represent the same physical attitude.

When $\mathbf{Z} = \mathbf{0}$, the marginalized attitude quaternion is equiprobable regardless of the correlation structure

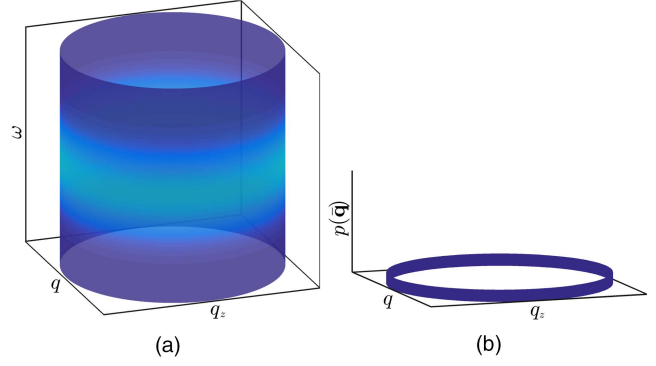


Fig. 4. Gauss-Bingham density on $\mathbb{R}^1 \times \mathbb{S}^1$ for $Z_1 = 0$. (a) Gauss-Bingham density. (b) Marginalized quaternion.

used. This is illustrated in Figs. 4(a) and 4(b), which show the Gauss-Bingham density in $\mathbb{R}^1 \times \mathbb{S}^1$ and the marginal density of the attitude quaternion when $Z_1 = 0$. This property of the Gauss-Bingham density is advantageous for representing the attitude quaternion as equiprobable when no prior attitude information is available.

A. Correlation Structure

In order to define the correlation structure for the orientation matrix $\mathbf{M}(\mathbf{z})$, it is important to note that $\mathbf{M}(\mathbf{z}) \in \text{SO}(s+1) \forall \mathbf{z} \in \mathbb{R}^r$. In order to ensure that this condition is met, the correlation structure is introduced into a minimum set of parameters necessary to specify the orientation matrix, denoted by $\phi(\mathbf{z})$, such that the orientation matrix is given by $\mathbf{M}(\phi(\mathbf{z}))$. A minimum parameter set, which is comprised of $s(s+1)/2 \triangleq n_\phi$ parameters, is necessary to define the orientation matrix; therefore $\phi(\mathbf{z}) \in \mathbb{R}^{s(s+1)/2}$ [24], [25]. The method for constructing the orientation matrix from the set of minimum parameters depends on s and the parameter set chosen. Methods for constructing the orientation matrix for dimensions $s = 1, 2, 3$ are presented in this section.

1) $s = 1$: First consider the Gauss-Bingham density specialized to $s = 1$. Only one parameter is necessary to specify the orientation matrix in this dimension since $n_\phi = 1$. This parameter is chosen to be the magnitude of the rotation about the known axis of rotation, which is given by $\theta(\mathbf{z})$, such that $\phi(\mathbf{z}) = \theta(\mathbf{z})$. The orientation matrix is then defined by

$$\mathbf{M}(\phi(\mathbf{z})) = \mathbf{M}(\theta(\mathbf{z})) = \begin{bmatrix} \cos \theta(\mathbf{z}) & \sin \theta(\mathbf{z}) \\ -\sin \theta(\mathbf{z}) & \cos \theta(\mathbf{z}) \end{bmatrix}.$$

The angle of rotation, $\theta(\mathbf{z})$, is defined on the interval $[-\pi, \pi)$ for all \mathbf{z} . Since $\mathbf{M}(\theta(\mathbf{z})) = \mathbf{M}(\theta(\mathbf{z}) + 2\pi k)$ for all $k \in \mathbb{Z}$, where \mathbb{Z} is the set of integers, $\theta(\mathbf{z})$ can be bounded to the interval $[-\pi, \pi)$ for all \mathbf{z} by adding the appropriate multiple of 2π .

2) $s = 2$: Now consider the Gauss-Bingham density specialized to $s = 2$. Three parameters are necessary to specify the orientation matrix in this dimension. These parameters are chosen to be the rotation vector, such

that $\phi(\mathbf{z}) = \theta(\mathbf{z})$. The orientation matrix is then given by (6) as

$$\begin{aligned} \mathbf{M}(\phi(\mathbf{z})) = \mathbf{M}(\theta(\mathbf{z})) = \mathbf{I} - \sin \|\theta(\mathbf{z})\| \left[\frac{\theta(\mathbf{z})}{\|\theta(\mathbf{z})\|} \times \right] \\ + (1 - \cos \|\theta(\mathbf{z})\|) \left[\frac{\theta(\mathbf{z})}{\|\theta(\mathbf{z})\|} \times \right]^2. \end{aligned}$$

If $\|\theta(\mathbf{z})\| = 0$, $\mathbf{M}(\mathbf{z}) = \mathbf{I}$, since the angle of rotation is zero. The norm of the rotation vector, $\|\theta(\mathbf{z})\|$, is defined on the interval $[-\pi, \pi)$ for all \mathbf{z} . Since $\mathbf{M}(\theta(\mathbf{z})) = \mathbf{M}(\theta(\mathbf{z}) + 2\pi k \theta(\mathbf{z}) / \|\theta(\mathbf{z})\|)$ for all $k \in \mathbb{Z}$, $\|\theta(\mathbf{z})\|$ can be bounded to the interval $[-\pi, \pi)$ for all \mathbf{z} by adding the appropriate multiple of $2\pi \theta(\mathbf{z}) / \|\theta(\mathbf{z})\|$.

3) $s = 3$: Finally, consider the Gauss-Bingham density specialized to $s = 3$. Six parameters are necessary to specify the orientation matrix in this dimension. These parameters are chosen to be two rotation vectors representing a left- and right-isoclonic rotation [26]. Let these rotation vectors be denoted by $\theta_L(\mathbf{z})$ and $\theta_R(\mathbf{z})$, respectively, such that $\phi(\mathbf{z}) = [\theta_L^T(\mathbf{z}) \ \theta_R^T(\mathbf{z})]^T$. The orientation matrix is then defined using left- and right-isoclonic rotations according to

$$\mathbf{M}(\phi(\mathbf{z})) = \mathbf{M} \left(\begin{bmatrix} \theta_L(\mathbf{z}) \\ \theta_R(\mathbf{z}) \end{bmatrix} \right) = \mathbf{L}(\bar{\mathbf{q}}(\theta_L(\mathbf{z}))) \mathbf{R}(\bar{\mathbf{q}}(\theta_R(\mathbf{z}))),$$

where

$$\begin{aligned} \mathbf{L}(\bar{\mathbf{q}}) &= \begin{bmatrix} q & -q_x & -q_y & -q_z \\ q_x & q & -q_z & q_y \\ q_y & q_z & q & -q_x \\ q_z & -q_y & q_x & q \end{bmatrix} \\ \mathbf{R}(\bar{\mathbf{q}}) &= \begin{bmatrix} q & -q_x & -q_y & -q_z \\ q_x & q & q_z & -q_y \\ q_y & -q_z & q & q_x \\ q_z & q_y & -q_x & q \end{bmatrix}, \end{aligned}$$

and $\bar{\mathbf{q}}(\theta_L(\mathbf{z}))$ and $\bar{\mathbf{q}}(\theta_R(\mathbf{z}))$ are defined by (7). The norm of each of these rotation vectors, $\|\theta_L(\mathbf{z})\|$ and $\|\theta_R(\mathbf{z})\|$, is defined on the interval $[-\pi, \pi)$ for all \mathbf{z} . Since

$$\mathbf{M} \left(\begin{bmatrix} \theta_L(\mathbf{z}) \\ \theta_R(\mathbf{z}) \end{bmatrix} \right) = \mathbf{M} \left(\begin{bmatrix} \theta_L(\mathbf{z}) + 2\pi k_L \theta_L(\mathbf{z}) / \|\theta_L(\mathbf{z})\| \\ \theta_R(\mathbf{z}) + 2\pi k_R \theta_R(\mathbf{z}) / \|\theta_R(\mathbf{z})\| \end{bmatrix} \right)$$

for all $k_L, k_R \in \mathbb{Z}$, $\|\theta_L(\mathbf{z})\|$ and $\|\theta_R(\mathbf{z})\|$ can be bounded to the interval $[-\pi, \pi)$ for all \mathbf{z} by adding the appropriate multiple of $2\pi \theta_L(\mathbf{z}) / \|\theta_L(\mathbf{z})\|$ and $2\pi \theta_R(\mathbf{z}) / \|\theta_R(\mathbf{z})\|$ to $\theta_L(\mathbf{z})$ and $\theta_R(\mathbf{z})$, respectively.

Now that the functional dependence of the orientation matrix, $\mathbf{M}(\phi(\mathbf{z}))$, on the minimal set of parameters, $\phi(\mathbf{z})$, has been defined for $s = 1, 2, 3$, the functional dependence of $\phi(\mathbf{z})$ on \mathbf{z} needs to be defined. Two choices for this functional dependence are considered: linear and quadratic. It is noted that the quadratic form of this functional dependence is not used after it is presented; however, it is a valid form of this functional

dependence and is presented to show the flexibility of the Gauss-Bingham density.

First, consider the quadratic dependence of $\phi(\mathbf{z})$ on \mathbf{z} , which is defined by

$$\begin{aligned} \phi(\mathbf{z}) = \phi_0 + \beta \mathbf{z} \\ + [\mathbf{z}^T \Gamma_1 \mathbf{z} \ \mathbf{z}^T \Gamma_2 \mathbf{z} \cdots \mathbf{z}^T \Gamma_{n_\phi} \mathbf{z}]^T, \end{aligned} \quad (25)$$

where $\phi_0 \in \mathbb{R}^{n_\phi}$, $\beta \in \mathbb{R}^{n_\phi \times r}$ and $\Gamma_i \in \{\mathbb{R}^{r \times r} : \Gamma_i = \Gamma_i^T\}$, $i = 1, \dots, n_\phi$ quantify the zeroth-, first-, and second-order correlation, respectively, of \mathbf{z} on $\phi(\mathbf{z})$. The choice of implementing \mathbf{z} instead of \mathbf{x} in the correlation structure results in nondimensional coefficients β and Γ_i , which is preferred for numerical stability. Noting that the orientation matrix $\mathbf{M}(\mathbf{z})$ is now explicitly defined by \mathbf{z} , ϕ_0 , β , $\Gamma_1, \dots, \Gamma_{n_\phi}$ and that \mathbf{z} is explicitly defined by \mathbf{x} , \mathbf{m} , and \mathbf{P} , the orientation matrix using the quadratic correlation structure is parameterized as

$$\mathbf{M}(\mathbf{z}) = \mathbf{M}(\mathbf{x}; \mathbf{m}, \mathbf{P}, \phi_0, \beta, \Gamma_1, \dots, \Gamma_{n_\phi}),$$

and the Gauss-Bingham density is given by the specialization of (23) as

$$\begin{aligned} p_{gb}(\mathbf{x}; \mathbf{m}, \mathbf{P}, \phi_0, \beta, \Gamma_1, \dots, \Gamma_{n_\phi}, \mathbf{Z}) = \\ p_g(\mathbf{x}; \mathbf{m}, \mathbf{P}) p_b(\bar{\mathbf{q}}; \mathbf{M}(\mathbf{x}; \mathbf{m}, \mathbf{P}, \phi_0, \beta, \Gamma_1, \dots, \Gamma_{n_\phi}), \mathbf{Z}). \end{aligned}$$

The number of parameters necessary to quantify the quadratic correlation between \mathbf{z} and $\phi(\mathbf{z})$ is $\frac{1}{2} n_\phi (2 + 2r + r(r + 1))$, which increases quadratically with r . For one-dimensional attitude ($\mathbb{R}^1 \times \mathbb{S}^1$), three-dimensional attitude ($\mathbb{R}^3 \times \mathbb{S}^3$), and dynamic pose ($\mathbb{R}^9 \times \mathbb{S}^3$) quantification, 3, 60, and 330 unique parameters are needed to quantify the quadratic relationship between $\phi(\mathbf{z})$ and \mathbf{z} .

Now, consider the linear correlation structure for $\phi(\mathbf{z})$, which is given by a simplification of (25) as

$$\phi(\mathbf{z}) = \phi_0 + \beta \mathbf{z}.$$

Using the linear correlation structure, the orientation matrix is parameterized as

$$\mathbf{M}(\mathbf{z}) = \mathbf{M}(\mathbf{x}; \mathbf{m}, \mathbf{P}, \phi_0, \beta),$$

and the Gauss-Bingham density is given by the specialization of (23) as

$$\begin{aligned} p_{gb}(\mathbf{x}; \mathbf{m}, \mathbf{P}, \phi_0, \beta, \mathbf{Z}) \\ = p_g(\mathbf{x}; \mathbf{m}, \mathbf{P}) p_b(\bar{\mathbf{q}}; \mathbf{M}(\mathbf{x}; \mathbf{m}, \mathbf{P}, \phi_0, \beta), \mathbf{Z}). \end{aligned}$$

The number of parameters necessary to quantify the linear correlation between \mathbf{z} and $\phi(\mathbf{z})$ is $n_\phi(1 + r)$, which increases linearly with r . For one-dimensional attitude, three-dimensional attitude, and dynamic pose quantification, 2, 24, and 60 unique parameters are needed to quantify the linear relationship between $\phi(\mathbf{z})$ and \mathbf{z} . Because the number of parameters necessary to quantify the linear correlation between \mathbf{z} and $\phi(\mathbf{z})$ increases linearly (as opposed to quadratically) with r , it is used in the remainder of this work.

B. Canonical Gauss-Bingham Density

The canonical Gauss-Bingham density is introduced by substituting the transformations

$$\mathbf{x} = \mathbf{S}\mathbf{z} + \mathbf{m} \quad \text{and} \quad \bar{\mathbf{q}} = \mathbf{M}(\mathbf{z})\bar{\mathbf{p}} \quad (26)$$

into (23), which yields the canonical Gauss-Bingham density as

$$\tilde{p}_{gb}(\mathbf{z}; \mathbf{Z}) = \tilde{p}_g(\mathbf{z})\tilde{p}_b(\bar{\mathbf{p}}; \mathbf{Z}),$$

where $\mathbf{z} = [\mathbf{z}^T \bar{\mathbf{p}}^T]^T$. The elements of \mathbf{z} are uncorrelated and zero mean, such that the covariance of \mathbf{z} is defined by \mathbf{I} and (17) and is given by

$$E_{\tilde{p}_{gb}}\{\mathbf{z}\mathbf{z}^T\} = \text{diag}[1 \cdots 1 \quad f_1 \cdots f_{s+1}]. \quad (27)$$

V. UNCERTAINTY PROPAGATION

In order to propagate the uncertainty of a given Gauss-Bingham-distributed state vector, an unscented transform is used and the weighted maximum log-likelihood parameters of the Gauss-Bingham density are found. The unscented transform generates a set of deterministically chosen sigma points that represent the given Gauss-Bingham density. Each sigma point is then transformed according to known (potentially) nonlinear system dynamics. The weighted maximum log-likelihood parameters of the propagated Gauss-Bingham density are then recovered from the transformed sigma points.

A. System Dynamics

Assume that discrete-time nonlinear system dynamics are given by

$$\mathbf{x}_k = \mathbf{f}(\mathbf{x}_{k-1}), \quad (28)$$

where $\mathbf{x} = [\mathbf{x}^T \bar{\mathbf{q}}^T]^T$, and define the state vector with the antipodal attitude quaternion as $\tilde{\mathbf{x}} = [\mathbf{x}^T \quad -\bar{\mathbf{q}}^T]^T$. Because $\bar{\mathbf{q}}$ quantifies an antipodally equivalent attitude representation in which $\bar{\mathbf{q}}$ and $-\bar{\mathbf{q}}$ represent the same physical attitude, the antipodal symmetry of $\bar{\mathbf{q}}$ must be preserved by the system dynamics; that is, if

$$\mathbf{x}_k = \mathbf{f}(\mathbf{x}_{k-1}) \quad \text{and} \quad \tilde{\mathbf{x}}_k = \mathbf{f}(\tilde{\mathbf{x}}_{k-1}), \quad (29)$$

then the quaternion elements of \mathbf{x}_k and $\tilde{\mathbf{x}}_k$ remain antipodal. Equation (29) defines an important property of the system dynamics, \mathbf{f} . This property states that the system dynamics preserve the antipodal symmetry of the quaternion, which is exploited to reduce the amount of computation necessary to propagate the sigma points representing the Gauss-Bingham density.

B. Unscented Transform

In order to select a set of weights and locations for the sigma points of the unscented transform for the canonical Gauss-Bingham density, the zeroth, first, and second moments between the canonical Gauss-Bingham density and the sigma points are matched in $\mathbb{R}^r \times \mathbb{R}^{s+1}$. The moments will be matched in $\mathbb{R}^r \times \mathbb{R}^{s+1}$; however, the sigma points will be parameterized such that they remain on the manifold $\mathbb{R}^r \times \mathbb{S}^s$. After finding sigma

points for the canonical Gauss-Bingham density, (26) is then used to convert the locations of the sigma points from the canonical Gauss-Bingham to the given Gauss-Bingham density.

In order to reduce the number of sigma points, only one of each pair of antipodal sigma points is considered and propagated since the system dynamics preserve the antipodal symmetry of the sigma points as shown by (29). To illustrate this concept, consider the following example antipodal sigma points in $\mathbb{R}^1 \times \mathbb{S}^1$ at t_{k-1} , \mathcal{X}_{k-1} and $\tilde{\mathcal{X}}_{k-1}$, that are antipodal in $\bar{\mathbf{q}}$ and given by

$$\mathcal{X}_{k-1} = \begin{bmatrix} 3 & \frac{1}{\sqrt{2}} & \frac{-1}{\sqrt{2}} \end{bmatrix}^T \quad \text{and} \\ \tilde{\mathcal{X}}_{k-1} = \begin{bmatrix} 3 & \frac{-1}{\sqrt{2}} & \frac{1}{\sqrt{2}} \end{bmatrix}^T.$$

These sigma points are propagated by some (potentially) nonlinear function, \mathbf{f} , that satisfies the property given by (29). Assume that this propagation transforms the sigma points to

$$\mathcal{X}_k = [4 \quad 0 \quad 1]^T \quad \text{and} \quad \tilde{\mathcal{X}}_k = [4 \quad 0 \quad -1]^T,$$

which are still antipodal in $\bar{\mathbf{q}}$; thus, the computational expense can be lowered by considering only \mathcal{X}_{k-1} . \mathcal{X}_{k-1} is transformed according to \mathbf{f} to obtain \mathcal{X}_k , and antipodal symmetry can be used to obtain $\tilde{\mathcal{X}}_k$, if desired.

In order to generate the sigma points for the Gauss-Bingham density, motivation is drawn from the $2n + 1$ unscented transform. The $2n + 1$ unscented transform for the canonical Gaussian density places two sigma points at equal but opposite deviations from zero for each of the $n = r$ canonical Gaussian states. A central sigma point is then placed at the origin. When generating sigma points for the canonical Gauss-Bingham density, which considers only one of each pair of antipodal points in the attitude quaternion, a similar approach to that of the $2n + 1$ unscented transform for the canonical Gaussian density is used.

In order to generate the sigma points for the canonical Gauss-Bingham density, first a set of sigma points that quantify deviations from the origin in each state of \mathbf{z} are introduced as $\pm\delta$ while $\bar{\mathbf{p}}$ is held constant as the identity quaternion. The locations of these $2r$ sigma points are given by

$$\mathcal{Z}^{(1),(2)} = \left[\overbrace{[\pm\delta \quad 0 \cdots 0]}^{\in \mathbb{R}^r} \quad \overbrace{[0 \cdots 0 \quad 1]}^{\in \mathbb{S}^s} \right]^T \\ \mathcal{Z}^{(3),(4)} = [0 \quad \pm\delta \cdots 0 \quad 0 \cdots 0 \quad 1]^T \\ \vdots \\ \mathcal{Z}^{(2r-1),(2r)} = [0 \cdots 0 \quad \pm\delta \quad 0 \cdots 0 \quad 1]^T,$$

with corresponding weights given by

$$w^{(1),(2)} = w^{(3),(4)} = \cdots = w^{(2r-1),(2r)} = \frac{w_g}{4r},$$

where $\mathcal{Z}^{(i),(j)}$ and $w^{(i),(j)}$ represent the locations and weights of the i th and j th sigma points, respectively, representing the canonical Gauss-Bingham density and w_g is a parameter used to specify the weights of these sigma points. The braces are used to denote the portions of \mathcal{Z} which are the Euclidean and quaternion states, respectively.

Next, angular deviations are introduced into the quaternion state as $\pm\alpha_\ell$ for $\ell = 1, 2, \dots, s$ while \mathbf{z} is held constant at zero in order to guarantee that the perturbed attitude quaternion remains on the unit hypersphere. These $2s$ sigma points are given by

$$\begin{aligned}\mathcal{Z}^{(2r+1),(2r+2)} &= \left[\overbrace{0 \dots 0}^{\in \mathbb{R}^r} \quad \overbrace{\pm S_{\alpha_1} \quad 0 \dots 0 \quad C_{\alpha_1}}^{\in \mathbb{S}^s} \right]^T \\ \mathcal{Z}^{(2r+3),(2r+4)} &= [0 \dots 0 \quad 0 \quad \pm S_{\alpha_2} \dots 0 \quad C_{\alpha_2}]^T \\ &\vdots \\ \mathcal{Z}^{(2r+2s-1),(2r+2s)} &= [0 \dots 0 \quad 0 \dots 0 \quad \pm S_{\alpha_s} \quad C_{\alpha_s}]^T,\end{aligned}$$

with corresponding weights given by

$$\begin{aligned}w^{(2r+1),(2r+2)} &= \frac{w_{b_1}}{4} \\ w^{(2r+3),(2r+4)} &= \frac{w_{b_2}}{4} \\ &\vdots \\ w^{(2r+2s-1),(2r+2s)} &= \frac{w_{b_s}}{4},\end{aligned}$$

where w_{b_ℓ} , for $\ell = 1, 2, \dots, s$, are parameters used to specify the weights of these sigma points and S_α and C_α represent the sine and cosine of α , respectively.

Finally, a central sigma point is placed at $\mathbf{z} = \mathbf{0}$ and in the “zero” direction of $\bar{\mathbf{p}}$, which is the identity quaternion. This single sigma point is given by

$$\mathcal{Z}^{(N)} = \left[\overbrace{0 \dots 0}^{\in \mathbb{R}^r} \quad \overbrace{0 \dots 0 \quad 1}^{\in \mathbb{S}^s} \right]^T,$$

with corresponding weight given by

$$w^{(N)} = \frac{w_c}{2},$$

where w_c is a parameter used to specify the weight of this sigma point and $N = 2r + 2s + 1$ is the total number of sigma points.

In order to find the parameters δ , α_ℓ , w_c , w_g , and w_{b_ℓ} , where $\ell = 1, 2, \dots, s$, which fully define the weights and locations of the sigma points for the canonical Gauss-Bingham density, the zeroth, first, and second moments between the sigma points and the canonical Gauss-Bingham density are matched. The zeroth and first moments of the canonical Gauss-Bingham are 1 and $\mathbf{0}$, respectively. The second moment of the canonical Gauss-Bingham density is given by (27). While only one of each antipodal pair of sigma points is stored and propagated, it is important to note that both of the

antipodal sigma points, which are equally weighted, are considered when calculating the moments of the sigma points. After accounting for the antipodal symmetry of each of the sigma points, the first moment of the sigma points is zero for any choice of the parameters. Matching the zeroth and second moments of the sigma points with the canonical Gauss-Bingham density yields

$$\sum_{\ell=1}^s w_{b_\ell} + w_c + w_g = 1 \quad (30a)$$

$$\frac{\delta^2 w_g}{r} = 1 \quad (30b)$$

$$w_{b_\ell} \sin^2 \alpha_\ell = f_\ell, \quad \ell = 1, 2, \dots, s \quad (30c)$$

$$\sum_{\ell=1}^s w_{b_\ell} \cos^2 \alpha_\ell + w_c + w_g = f_{s+1}, \quad (30d)$$

where (30a) stems from the zeroth moment and (30b)–(30d) stem from the second moment. Summing (30c) for $\ell = 1, 2, \dots, s$ and (30d) while noting the properties in (18) yields (30a); thus, (30d) is redundant and may be neglected. Solving (30b) and (30c) for δ and α_ℓ gives the locations of the sigma points as a function of their weights as

$$\delta = \sqrt{\frac{r}{w_g}} \quad \text{and} \quad \alpha_\ell = \text{asin} \sqrt{\frac{f_\ell}{w_{b_\ell}}}, \quad (31)$$

where $\ell = 1, 2, \dots, s$. Now, the weights must be selected for the sigma points. In order for (31) to have real solutions, w_{b_ℓ} must be greater than or equal to f_ℓ for all $\ell = 1, 2, \dots, s$. In order to ensure that this condition is met, a somewhat nonintuitive choice for the weights of the sigma points for the canonical Gauss-Bingham density is chosen that parallels the choice of weights of the sigma points for the Bingham density presented in [12]. Noting the properties given in (18), the weights of the sigma points representing the Gauss-Bingham density which satisfy (30a) are chosen as

$$w_{b_\ell} = f_\ell + (1 - \lambda - \kappa) \frac{f_{s+1}}{s}, \quad \ell = 1, 2, \dots, s \quad (32a)$$

$$w_c = \lambda f_{s+1} \quad (32b)$$

$$w_g = \kappa f_{s+1}, \quad (32c)$$

where λ and κ are positive tuning parameters such that $\lambda + \kappa < 1$. While choosing the weights according to (32) is nonintuitive, this choice of weights satisfies (30a) and provides real locations for the sigma points. λ and κ are chosen such that the weights of all the sigma points approach an equal weight of $1/N$ as the uncertainty in the states corresponding to $\bar{\mathbf{q}}$ approaches zero; that is, $Z_1, Z_2, \dots, Z_s \rightarrow -\infty$. This choice of weights ensures that the sigma points possess nearly equal weights, and thus have nearly equal importance, when the uncertainty in the attitude quaternion is small. Using the properties in (18), the λ and κ that yield equal weights for the sigma

points as the uncertainty in the quaternion goes to zero are given by

$$\lambda = \frac{1}{N} \quad \text{and} \quad \kappa = \frac{2r}{N}. \quad (33)$$

The sigma points on the canonical Gauss-Bingham density, which are defined in terms of the parameters in (31), (32), and (33), are transformed from the canonical Gauss-Bingham density to the Gauss-Bingham density of interest defined by $p_{gb}(\mathbf{x}; \mathbf{m}, \mathbf{P}, \phi_0, \beta, \mathbf{Z})$ according to (26). These transformed sigma points and their associated weights are denoted by $\mathcal{X}^{(i)}$ and $w^{(i)}$, respectively, where $i = 1, 2, \dots, N$.

The sigma points representing the Gauss-Bingham density at t_{k-1} , \mathcal{X}_{k-1} , are then transformed according to the nonlinear system dynamics given by (28) to obtain the sigma points representing the Gauss-Bingham density at t_k , \mathcal{X}_k . If the dynamical system is governed by continuous-time dynamics, the nonlinear discrete-time function in (28), f , is given by the integration of \mathbf{x}_{k-1} from t_{k-1} to t_k to obtain \mathbf{x}_k .

C. Maximum Weighted Log-Likelihood Gauss-Bingham Parameters

In order to obtain the parameters of the best-fit Gauss-Bingham density given the set of sigma points and weights at t_k , the parameters of the Gauss-Bingham density that maximize the weighted log-likelihood of the sigma points are found. To illustrate why the maximum weighted log-likelihood parameters are sought, consider the case when the unscented transform is used for a state that exists in \mathbb{R}^r . Given the sigma points and weights from the unscented transform, the mean and covariance are recovered from the weighted sample mean and covariance of the sigma points. It can be shown that the weighted sample mean and covariance of the sigma points is the mean and covariance of the Gaussian density that maximizes the weighted log-likelihood of the sigma points.

In this spirit, the parameters of the Gauss-Bingham density are recovered from the sigma points according to

$$\mathbf{m}_k, \mathbf{P}_k, \phi_{0,k}, \beta_k, \mathbf{Z}_k = \underset{\mathbf{m}, \mathbf{P}, \phi_0, \beta, \mathbf{Z}}{\operatorname{argmax}} \sum_{i=1}^N w^{(i)} \ln p_{gb}(\mathcal{X}_k^{(i)}; \mathbf{m}, \mathbf{P}, \phi_0, \beta, \mathbf{Z}). \quad (34)$$

This maximization can be performed analytically for the mean and covariance of the Gaussian density, \mathbf{m} and \mathbf{P} . First, note that the sigma points can be decomposed into their Euclidean and quaternion portions according to $\mathcal{X}_k = [\mathcal{X}_{x,k}^T \quad \mathcal{X}_{q,k}^T]^T$. The mean and covariance of the Gaussian density that maximizes the weighted

log-likelihood of the sigma points is given by the sample mean and covariance of the Euclidean portion of the sigma points according to

$$\mathbf{m}_k = 2 \sum_{i=1}^N w^{(i)} \mathcal{X}_{x,k}^{(i)} \quad (35a)$$

$$\mathbf{P}_k = 2 \sum_{i=1}^N w^{(i)} (\mathcal{X}_{x,k}^{(i)} - \mathbf{m}_k)(\mathcal{X}_{x,k}^{(i)} - \mathbf{m}_k)^T, \quad (35b)$$

where the factor of two is included since only one of each antipodal pair of sigma points in the quaternion state is quantified.

After using (35) to determine \mathbf{m}_k and \mathbf{P}_k , (34) becomes

$$\phi_{0,k}, \beta_k, \mathbf{Z}_k = \underset{\phi_0, \beta, \mathbf{Z}}{\operatorname{argmax}} J(\phi_0, \beta, \mathbf{Z}), \quad (36)$$

where

$$J(\phi_0, \beta, \mathbf{Z}) = \sum_{i=1}^N w^{(i)} \ln p_{gb}(\mathcal{X}_k^{(i)}; \mathbf{m}_k, \mathbf{P}_k, \phi_0, \beta, \mathbf{Z}).$$

This maximization is carried out numerically to find ϕ_0 , β , and \mathbf{Z} . In order to perform this numerical maximization, it is first transformed into a root-finding problem according to the first derivative conditions of a maximum, i.e.

$$\frac{\partial J(\phi_{0,k}, \beta_k, \mathbf{Z}_k)}{\partial \phi_{0,k}} = \mathbf{0} \quad (37a)$$

$$\frac{\partial J(\phi_{0,k}, \beta_k, \mathbf{Z}_k)}{\partial \beta_k} = \mathbf{0} \quad (37b)$$

$$\frac{\partial J(\phi_{0,k}, \beta_k, \mathbf{Z}_k)}{\partial \mathbf{Z}_k} = \mathbf{0}, \quad (37c)$$

where the explicit expressions for the derivatives are omitted for brevity. A root-finding algorithm is used to find the $\phi_{0,k}$, β_k , and \mathbf{Z}_k that satisfy (37). To initialize the root-finding algorithm, $\phi_{0,k-1}$, β_{k-1} , and \mathbf{Z}_{k-1} are used. By initializing the root-finding algorithm in this way, if the propagation time step is chosen sufficiently small, $\phi_{0,k-1}$, β_{k-1} , and \mathbf{Z}_{k-1} remain close to the local maximum and a gradient-based root-finding algorithm will converge to $\phi_{0,k}$, β_k , and \mathbf{Z}_k without excessive iteration required or risk of diverging to a different root.

A number of root-finding algorithms can be used to find the $\phi_{0,k}$, β_k , and \mathbf{Z}_k that satisfy (37). The Levenberg-Marquardt algorithm, a well-known optimizer, is chosen to find these $\phi_{0,k}$, β_k , and \mathbf{Z}_k [27], [28]. This algorithm is used to find the roots of an arbitrary system of equations defined by $\mathbf{g}(\mathbf{x}) = \mathbf{0}$ by minimizing the cost function $\mathbf{g}^T(\mathbf{x})\mathbf{g}(\mathbf{x})$ using \mathbf{x} as the minimization variable. The Levenberg-Marquardt algorithm was chosen to find $\phi_{0,k}$, β_k , and \mathbf{Z}_k since the cost function will remain near the minimum if the time step is chosen sufficiently small and $\phi_{0,k-1}$, β_{k-1} , and \mathbf{Z}_{k-1} are used

to initialize the algorithm. Applying the Levenberg-Marquardt algorithm in this manner to find the roots of (37) was found to be more computationally efficient than applying it to the optimization problem in (36) directly.

D. Uncertainty Propagation Algorithm

In summary, the algorithm used to propagate the Gauss-Bingham density is given by

— Given:

- A Gauss-Bingham-distributed state vector at t_0 defined by $p_{gb}(\mathbf{x}; \mathbf{m}_0, \mathbf{P}_0, \phi_{0,0}, \beta_0, \mathbf{Z}_0)$.
- System dynamics that preserve the antipodal symmetry of the quaternion as defined by the property given by (29).
- A sequence of times to which to propagate the Gauss-Bingham density, t_1, t_2, \dots, t_f .

- 1) Generate the sigma points and weights according to $p_{gb}(\mathbf{x}; \mathbf{m}_0, \mathbf{P}_0, \phi_{0,0}, \beta_0, \mathbf{Z}_0)$.
- 2) Set the time counter to $k = 1$
- 3) Propagate the sigma points from t_{k-1} to t_k according to the given system dynamics.
- 4) Recover \mathbf{m}_k and \mathbf{P}_k according to (35).
- 5) Recover $\phi_{0,k}$, β_k , and \mathbf{Z}_k according to the root-finding problem defined by (37) using $\phi_{0,k-1}$, β_{k-1} , and \mathbf{Z}_{k-1} to initialize the root-finding algorithm.
- 6) If $t_k = t_f$, stop; if $t_k < t_f$, set $k = k + 1$ and return to step 3.

The sequence of times to which to propagate the Gauss-Bingham density, t_1, t_2, \dots, t_f , should be chosen such that the time step is small enough that $\phi_{0,k-1}$, β_{k-1} , and \mathbf{Z}_{k-1} are close to $\phi_{0,k}$, β_k , and \mathbf{Z}_k in order to ensure that the root-finding algorithm converges to the proper solution for $\phi_{0,k}$, β_k , and \mathbf{Z}_k . The size of the time step is a compromise between computational cost and ensuring that the root-finding algorithm converges to the correct root. Because the sigma points are not resampled at each time step, no approximation error is introduced by choosing the time step too small. Since the time step chosen is problem dependent, general guidelines for choosing this time step can not be imposed.

VI. SIMULATIONS

Two simulations are performed to illustrate uncertainty propagation using the Gauss-Bingham density. The first simulation propagates the uncertainty of the planar attitude and angular velocity of a body in $\mathbb{R}^1 \times \mathbb{S}^1$, where the Gauss-Bingham density can be visualized on the unit cylinder. This simulation provides an intuitive example of uncertainty propagation using the Gauss-Bingham density. The second simulation propagates the uncertainty in the dynamic pose (position, velocity, attitude, and angular velocity) of a chase spacecraft with respect to a target spacecraft. This simulation compares uncertainty propagation using the Gauss-Bingham

density to the predictor of the multiplicative extended Kalman filter and a Monte Carlo approach in order to show the efficacy of uncertainty propagation using the Gauss-Bingham density.

A. Planar Attitude and Angular Velocity

Consider the attitude quaternion and angular velocity representing the one-dimensional attitude motion of a body undergoing rotation about the z -axis. In this case, the state vector of the body is defined by (24). The angular velocity comprises the Gaussian-distributed portion of the state vector, with initial mean and covariance given by

$$\mathbf{m}_0 = 0 \quad \text{and} \quad \mathbf{P}_0 = (0.01^\circ/\text{s})^2, \quad (38)$$

respectively. The attitude quaternion comprises the conditional Bingham-distributed portion of the state vector, and is initially uncorrelated with the angular velocity (that is, $\beta_0 = 0$). The parameters defining the orientation and concentration of the conditional Bingham-distributed portion of the state vector are given by

$$\phi_0 = 0 \quad \text{and} \quad Z_{1,0} = -100,$$

respectively. The Gauss-Bingham density representing the initial attitude quaternion and angular velocity of the body, as well as the sigma points generated by the unscented transform, are shown in Fig. 5(a). The marginalized density of the initial attitude quaternion is shown in Fig. 5(c).

The body undergoes torque-free motion, that is, $\tau^B = 0$. The temporal evolution of the attitude quaternion and angular velocity are given by (9) and (10), respectively. The uncertainty propagation algorithm summarized in Section V-D is used to propagate the uncertainty of the attitude quaternion and angular velocity forward in time. A time step of one minute is used to propagate the uncertainty, which is small enough to ensure that the root-finding algorithm converges to the proper $\phi_{0,k}$, β_k , and \mathbf{Z}_k at each time step. Fig. 5 shows the evolution of Gauss-Bingham density and sigma points representing the attitude quaternion and angular velocity of the body, as well as the marginalized density of the attitude quaternion over time. Table I provides the corresponding parameters of the Gauss-Bingham density over time. It is observed that the mean and covariance of the angular velocity, \mathbf{m} and \mathbf{P} , respectively, remain constant, which is expected since (10) shows that the angular-velocity is constant under torque-free motion.

The concentration parameter of the conditional Bingham density, \mathbf{Z} , remains constant (within numerical accuracy of the root finding algorithm). The mean direction of the Gauss-Bingham density, ϕ_0 , remains at zero since the mean of the angular velocity is zero for all time; however the linear correlation parameter, β evolves in time in order to quantify the effect of the uncertain angular velocity on the attitude quaternion.

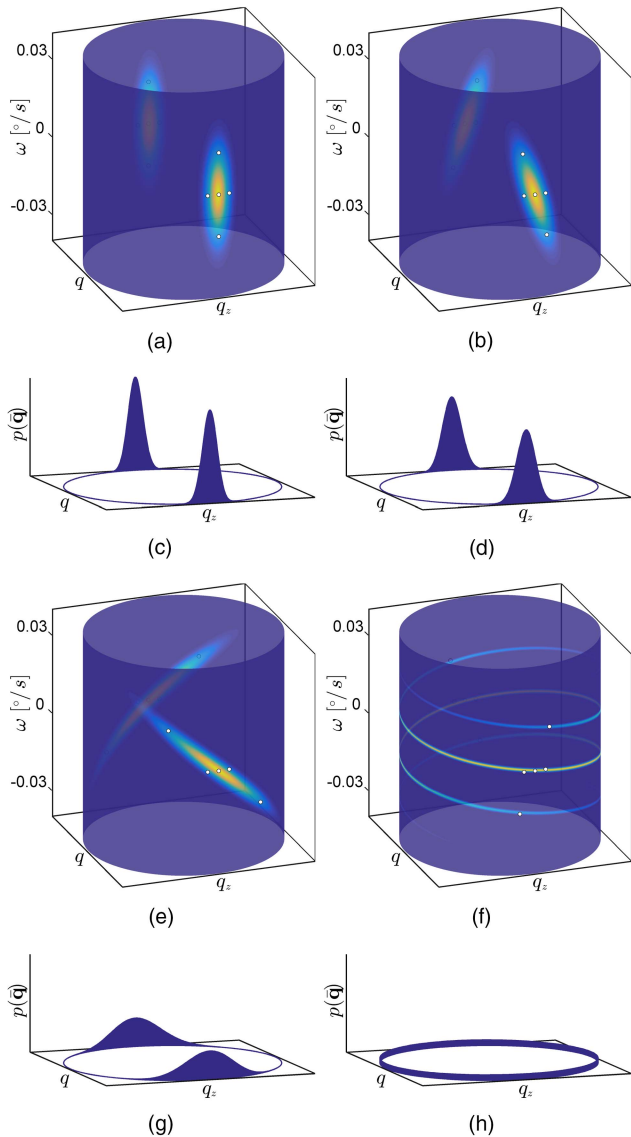


Fig. 5. Gauss-Bingham uncertainty propagation for one-dimensional attitude motion. (a) Initial state density. (b) State density at 15 minutes. (c) Initial quaternion density. (d) Quaternion density at 15 minutes. (e) State density at 1 hour. (f) State density at 6 hours. (g) Quaternion density at 1 hour. (h) Quaternion density at 6 hours.

TABLE I
Gauss-Bingham Parameters over time

Time [hours]	m [$^{\circ}/s$]	P [$(^{\circ}/s)^2$]	ϕ_0	β	Z_1
0	0	$(0.01)^2$	0	0.0000	-100
0.25	0	$(0.01)^2$	0	0.0785	-100
1	0	$(0.01)^2$	0	0.3142	-100
6	0	$(0.01)^2$	0	1.8850	-100

It is interesting to note that β evolves linearly in time for this problem. The Gauss-Bingham density eventually wraps around its cylindrical manifold as it is propagated, which causes the attitude quaternion to become equiprobable as time increases, and is apparent in Fig. 5(h). This is an expected result for a body undergoing

one-dimensional attitude motion with an uncertain angular velocity; as time increases, the uncertainty in the attitude quaternion of the body grows until the attitude quaternion becomes equiprobable.

Several important properties of the Gauss-Bingham density and its utility in uncertainty propagation can be observed in Fig. 5. The Gauss-Bingham density is antipodally symmetric in the quaternion state for all time, which is a necessary property to properly quantify the uncertainty in the attitude quaternion. Since this example quantifies the one-dimensional attitude motion in $\mathbb{R}^1 \times \mathbb{S}^1$, $N = 5$ sigma points are required to quantify the temporal evolution of the Gauss-Bingham density. The attitude quaternion becomes equiprobable as the uncertainty is propagated; however, the concentration parameter Z_1 does not approach zero. As the uncertainty is propagated, the attitude quaternion becomes equiprobable due to the wrapping of the Gauss-Bingham density around the cylinder, not because the concentration parameter approaches zero.

B. Spacecraft Relative Pose

Now consider an example in which a chase spacecraft is orbiting in close proximity to a target spacecraft. The state of the chase spacecraft is defined to be $[\omega^T \ \delta r^T \ \delta v^T \ \bar{q}^T]^T$, where \bar{q} and ω represent the attitude quaternion and angular velocity of the chase spacecraft, respectively, and δr and δv represent the relative position and velocity, respectively, of the chase spacecraft with respect to the target spacecraft. The chase spacecraft is taken to have an identity inertia tensor and undergoes torque-free motion, with the temporal evolution of the attitude quaternion and angular velocity given by (9) and (10), respectively. Since the body undergoes torque-free motion and has an identity inertia tensor, (10) shows that the angular velocity is constant in time.

In order to quantify the temporal evolution of the relative position and velocity, the Clohessy-Wiltshire equations are used [29]–[31]. The Clohessy-Wiltshire equations approximate the relative motion of the chase spacecraft with respect to the target spacecraft under the assumptions that the spacecraft are in close proximity and that the target spacecraft is in a circular orbit. If these assumptions are valid, the Clohessy-Wiltshire equations governing the temporal evolution of the relative position and velocity are

$$\begin{bmatrix} \delta \dot{r} \\ \delta \dot{v} \end{bmatrix} = \begin{bmatrix} 0 & 0 & 0 & 1 & 0 & 0 \\ 0 & 0 & 0 & 0 & 1 & 0 \\ 0 & 0 & 0 & 0 & 0 & 1 \\ 3n^2 & 0 & 0 & 0 & 2n & 0 \\ 0 & 0 & 0 & -2n & 0 & 0 \\ 0 & 0 & -n^2 & 0 & 0 & 0 \end{bmatrix} \begin{bmatrix} \delta r \\ \delta v \end{bmatrix}, \quad (39)$$

where n is the mean motion of the target spacecraft and δr and δv are expressed in a rotating coordinate frame centered on the target spacecraft. The rotating

coordinate frame is defined by the position and velocity vectors of the target spacecraft. The target spacecraft is taken to be in a geostationary orbit with an orbital radius of 42164 km, which results in a mean motion of the target spacecraft of 7.2920×10^{-5} rad/s.

The Gauss-Bingham density is used to quantify the uncertainty of the state vector of the chase spacecraft. The Gaussian portion of the Gauss-Bingham density quantifies the uncertainty of the angular velocity, relative position, and relative velocity, with initial mean and covariance given by

$$\mathbf{m}_0 = \begin{bmatrix} 0.5^\circ/\text{s} \\ 0.8^\circ/\text{s} \\ 1.0^\circ/\text{s} \\ 0 \\ 10 \text{ km} \\ 0 \\ 0 \\ 0 \\ 0 \\ 0 \end{bmatrix} \quad \text{and} \quad \mathbf{P}_0 = \text{diag} \begin{bmatrix} 0.1^2 (\text{ }^\circ/\text{s})^2 \\ 0.1^2 (\text{ }^\circ/\text{s})^2 \\ 0.1^2 (\text{ }^\circ/\text{s})^2 \\ 1 \text{ m}^2 \\ 1 \text{ m}^2 \\ 1 \text{ m}^2 \\ 0.01^2 (\text{m/s})^2 \\ 0.01^2 (\text{m/s})^2 \\ 0.01^2 (\text{m/s})^2 \end{bmatrix}^T, \quad (40)$$

respectively. The attitude quaternion of the chase spacecraft comprises the conditional Bingham-distributed portion of the state vector, and is initially uncorrelated with the angular velocity, relative position, and relative velocity (that is, $\beta_0 = \mathbf{0}$). The parameters defining the initial orientation and concentration of the conditional Bingham-distributed portion of the state vector are given by

$$\phi_0 = \mathbf{0} \quad \text{and} \quad Z_{1,0} = Z_{2,0} = Z_{3,0} = -5000,$$

respectively.

The uncertainty propagation algorithm summarized in Section V-D is used to propagate the uncertainty of the angular velocity, relative position, relative velocity, and attitude quaternion forward in time. A time step of fifteen seconds is used to propagate the uncertainty, which is small enough to ensure that the root-finding algorithm converges to the proper $\phi_{0,k}$, β_k , and \mathbf{Z}_k at each time step. Uncertainty propagation using the Gauss-Bingham density is compared to two other methods of uncertainty propagation to evaluate its efficacy: a Monte Carlo approach and the predictor step of the multiplicative extended Kalman filter (MEKF) [5], [32], [33]. 100,000 Monte Carlo samples are realized from the initial Gauss-Bingham density using an acceptance sampling method, and are propagated forward in time to quantitatively represent the true evolution of the initial Gauss-Bingham density.

The predictor step of the MEKF quantifies the “mean” using the attitude quaternion and relies on a small angle assumption to project the uncertainty in the

attitude quaternion into a three parameter attitude representation (the rotation vector is used in this analysis). Quotation marks are used around “mean” for the MEKF to indicate that it is not the mean as defined by the first moment of the state vector; rather, it is the “mean” quaternion as defined by one of the antipodal pair used to quantify the quaternion estimate. In order to find the equivalent “mean” and covariance for the MEKF given the initial Gauss-Bingham density, it is first noted that “mean” attitude quaternion is the identity quaternion since $\phi_0 = \mathbf{0}$ and $\beta_0 = \mathbf{0}$; thus, the mean for the MEKF is given by the concatenation of the mean given in (40) and the identity quaternion. The equivalent covariance of the MEKF state vector, which is expressed using the rotation vector instead of the attitude quaternion, is found by converting the quaternion portion of the initial Monte Carlo samples to their equivalent rotation vector according to (8), and calculating their sample covariance.

Since the angular velocity, relative position, and relative velocity are initially Gaussian-distributed, evolve according to linear dynamics, and their temporal evolution is not a function of the attitude quaternion, they remain Gaussian-distributed for all time. Because of this, both the Gauss-Bingham and MEKF uncertainty propagation methods perfectly capture the evolution of the uncertainty in these states, which is presented in Figs. 6–8 and shows the standard deviation of each component of these states quantified by both the MEKF and the Gauss-Bingham density over time. Furthermore, the mean of these quantities is constant for all time since their mean is a stationary solution to (10) and (39) under torque-free motion with an identity inertia tensor. Fig. 6 shows that the uncertainty of the angular velocity is constant, as expected since the angular velocity is constant. Fig. 7 shows that the uncertainty in the relative position grows as time increases. Fig. 8 shows that the uncertainty in the x - and y -components of the relative velocity increase, while the uncertainty in the z -component decreases. This decrease in uncertainty is expected due to the periodicity present in the Clohessy-Wiltshire equations. If the uncertainty is propagated for an entire orbit of the target spacecraft (approximately 24 hours), it would complete one cycle of its period.

Uncertainty propagation using the Gauss-Bingham density does not require that the system dynamics governing the Gaussian-distributed states be linear nor that their temporal evolution be functionally independent of the attitude quaternion. These conditions are used in this example to simplify the presentation and analysis of the results of the uncertainty propagation. If nonlinear system dynamics are used, or if the system dynamics are a function of the attitude quaternion, the best-fit Gaussian density that maximizes the weighted log-likelihood of the sigma points as defined by (35) is found.

Because the attitude uncertainty quantified by the Gauss-Bingham density and Monte Carlo samples are

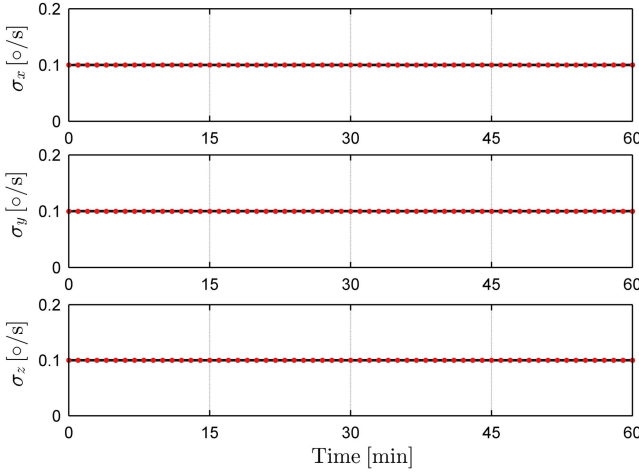


Fig. 6. Gaussian-distributed angular velocity standard deviation quantified by the Gauss-Bingham density (black) and the MEKF (red).

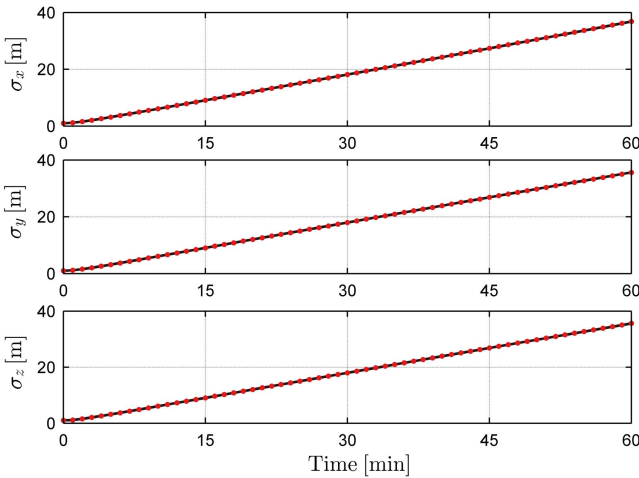


Fig. 7. Gaussian-distributed relative position standard deviation quantified by the Gauss-Bingham density (black) and the MEKF (red).

expressed using the attitude quaternion and the uncertainty quantified by the MEKF predictor is expressed using the rotation vector, the uncertainty quantified by the Gauss-Bingham density and Monte Carlo samples are converted to rotation vector space in order to make a direct comparison. The rotation vector space is chosen for this comparison since it is a three parameter representation of attitude. In order to convert the uncertainty quantified by the Gauss-Bingham density and Monte Carlo samples from the attitude quaternion representation to the rotation vector representation, first, 100,000 samples of the Gauss-Bingham density are generated using an acceptance sampling method. The quaternion portion of the Gauss-Bingham samples, as well as the Monte Carlo samples, are then converted to their equivalent rotation vector according to (8). Expectation maximization [34] is then performed for each set of samples to fit a Gaussian mixture density to the x - y , y - z , and x - z projections of the rotation vector portion of the respec-

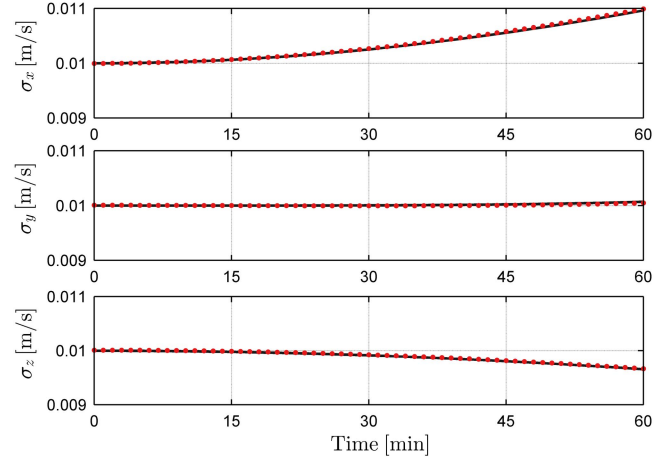


Fig. 8. Gaussian-distributed relative velocity standard deviation quantified by the Gauss-Bingham density (black) and the MEKF (red).

tive samples. This process is used *only* to visualize the uncertainty of the attitude quaternion quantified by the Gauss-Bingham density and the Monte Carlo samples in rotation vector space, and is not an element of the uncertainty propagation using the Gauss-Bingham density. Because the MEKF quantifies the mean and covariance of the rotation vector and not its density, the density is assumed to be Gaussian.

The attitude uncertainty quantified by the Gauss-Bingham density, Monte Carlo samples, and MEKF at a time of five minutes are presented in Fig. 9. Figs. 9(a) and 9(b) show the x - y projection of the rotation vector for 1,000 of the Monte Carlo and Gauss-Bingham samples, as well as the Gaussian mixture densities fit to these samples to show the agreement between the samples and the densities. These plots are repeated without the samples in Figs. 9(c) and 9(d) for clarity along with the uncertainty quantified by the MEKF in red in Fig. 9(d). Figs. 9(e) and 9(f) and Figs. 9(g) and 9(h) show the y - z and x - z projections, respectively, of the uncertainty quantified by the Gauss-Bingham density, true density (as approximated from the Monte Carlo samples), and MEKF. At the time of five minutes, the Gauss-Bingham density agrees very well with the true density. The MEKF quantifies the mean and covariance of the true density as well, which is attributed to the fact that the attitude uncertainty is still relatively small at this time.

Fig. 10 shows the uncertainty quantified by the Gauss-Bingham density, true density (as approximated from the Monte Carlo samples), and MEKF at a time of one hour in the same plots as Fig. 9. After propagating the uncertainty for one hour, the attitude uncertainty quantified by the MEKF does not agree with the true uncertainty, as it has outgrown the $\|\theta\| \in [-\pi, \pi]$ bound on the rotation vector. This uncertainty can potentially be wrapped such that it is expressed in the appropriate bounded region; however, this is not common practice when using the MEKF. The underlying small angle

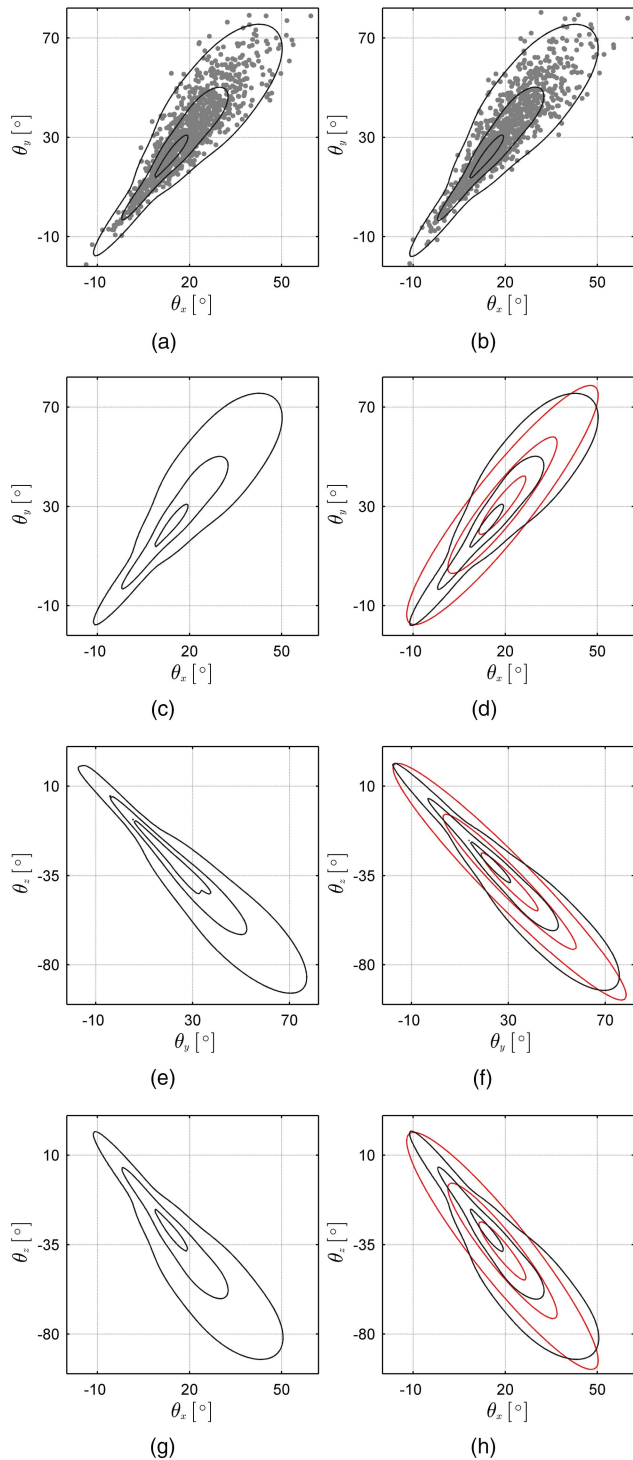


Fig. 9. True, Gauss-Bingham (GB), and MEKF attitude uncertainties expressed in rotation vector space at a time of five minutes. The MEKF density is shown in red. (a) True θ_x - θ_y density and samples. (b) GB θ_x - θ_y density and samples. (c) True θ_x - θ_y density. (d) GB and MEKF θ_x - θ_y densities. (e) True θ_y - θ_z density. (f) GB and MEKF θ_y - θ_z densities. (g) True θ_x - θ_z density. (h) GB and MEKF θ_x - θ_z densities.

assumption used to derive the predictor of the MEKF becomes invalid when the attitude uncertainties become large; thus, it is not well-suited to propagate large attitude uncertainties. This can be observed by noting that, even if the uncertainty were wrapped to the appropriate

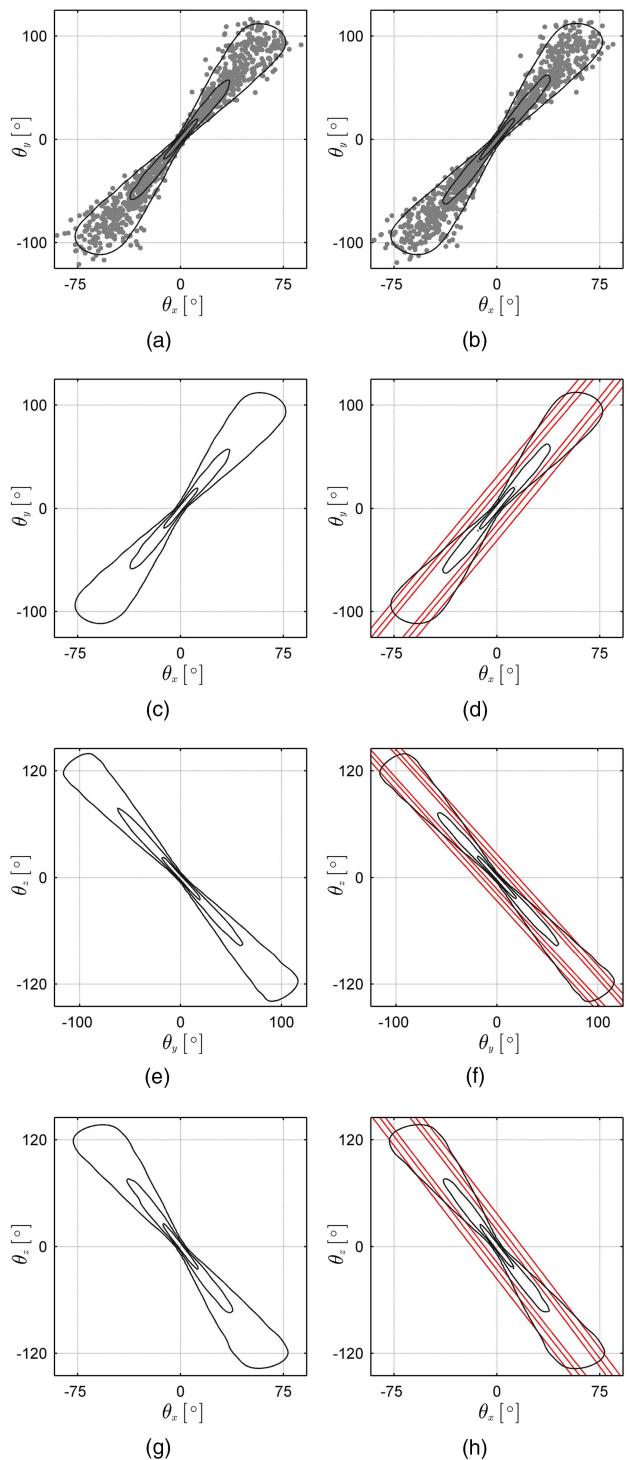


Fig. 10. True, Gauss-Bingham (GB), and MEKF attitude uncertainties expressed in rotation vector space at a time of one hour. The MEKF density is shown in red. (a) True θ_x - θ_y density and samples. (b) GB θ_x - θ_y density and samples. (c) True θ_x - θ_y density. (d) GB and MEKF θ_x - θ_y densities. (e) True θ_y - θ_z density. (f) GB and MEKF θ_y - θ_z densities. (g) True θ_x - θ_z density. (h) GB and MEKF θ_x - θ_z densities.

boundary, it still will not possess the appropriate hour-glass shape as the true density does.

After propagating the uncertainty for one hour, the Gauss-Bingham density is still in close agreement with the true density as is shown in Fig. 10. This is due

to the fact that the uncertainty propagation using the Gauss-Bingham density does not rely on a small angle assumption. The uncertainty is also quantified on the natural manifold of the attitude quaternion and the other Euclidean states, $\mathbb{R}^9 \times \mathbb{S}^3$, so the uncertainty cannot escape the bounded region on which it is defined. Because of these reasons, uncertainty propagation using the Gauss-Bingham density remains well-suited to quantify attitude uncertainty, even as the attitude uncertainty becomes large.

VII. CONCLUSIONS

A new probability density function, called the Gauss-Bingham density, was proposed that represents the uncertainty of an attitude quaternion and other Euclidean states of a body under a common probabilistic framework. The proposed Gauss-Bingham density is constructed as the product of a Gaussian density and a Bingham density that is conditioned on the Gaussian-distributed random variable, which quantifies the correlation between the quaternion and Euclidean states and exists on their natural manifold, $\mathbb{R}^r \times \mathbb{S}^s$. The Gauss-Bingham density quantifies a uniformly-distributed quaternion when its concentration matrix is null, which provides a convenient method to initialize the uncertainty when no attitude information is available. Uncertainty propagation using the Gauss-Bingham density was presented, which leverages an unscented transformation and recovers the maximum weighted log-likelihood parameters of the Gauss-Bingham density from the sigma points. The Gauss-Bingham density properly quantifies the uncertainty of the attitude quaternion and other Euclidean states without relying on a small-angle assumption to project the uncertainty in the attitude quaternion into a three parameter attitude representation, as does the predictor of the multiplicative extended Kalman filter (MEKF). Since the uncertainty is quantified on its natural manifold, it is not possible for the uncertainty propagated using the Gauss-Bingham density to outgrow its bounds like the predictor of the MEKF.

Two simulations were presented. The first simulation showed how the Gauss-Bingham density can be used to propagate the uncertainty of the one-dimensional attitude quaternion and angular velocity of a body where a convenient visualization of the uncertainty exists on $\mathbb{R}^1 \times \mathbb{S}^1$. As the uncertainty was propagated, it wraps around the cylinder defined by $\mathbb{R}^1 \times \mathbb{S}^1$, and the attitude quaternion becomes equiprobable, as expected. The second simulation showed how the Gauss-Bingham density can be used to propagate the uncertainty of the three-dimensional attitude quaternion, angular velocity, relative position, and relative velocity of a chase spacecraft about a target spacecraft. This simulation compared uncertainty propagation using the Gauss-Bingham to that of the predictor of the MEKF and a Monte Carlo approach. When the attitude uncertainty became large,

the uncertainty quantified by the Gauss-Bingham density remained in close agreement with the true density, where that of the MEKF did not.

REFERENCES

- [1] G. Stienne, S. Reboul, M. Azmani, J. B. Choquel, and M. Benjelloun
A multi-temporal multi-sensor circular fusion filter,
Information Fusion, vol. 18, pp. 86–100, 2014.
- [2] G. Kurz, I. Gilitschenski, and U. D. Hanebeck
Recursive Bayesian filtering in circular state spaces,
CoRR, vol. abs/1501.05151, 2015.
- [3] K. V. Mardia and T. W. Sutton
A model for cylindrical variables with applications,
Journal of the Royal Statistical Society. Series B (Methodological), vol. 40, no. 2, pp. 229–233, 1978.
- [4] J. T. Horwood and A. B. Poore
Gauss von Mises distribution for improved uncertainty realism in space situational awareness,
SIAM/ASA Journal of Uncertainty Quantification, vol. 2, pp. 276–304, 2014.
- [5] F. L. Markley and J. L. Crassidis
Fundamentals of Spacecraft Attitude Determination and Control.
Springer, 2014.
- [6] M. D. Shuster
A survey of attitude representations,
The Journal of the Astronautical Sciences, vol. 41, no. 4, pp. 439–517, October–December 1993.
- [7] P. C. Hughes
Spacecraft Attitude Dynamics.
John Wiley & Sons, 1986.
- [8] C. Bingham
An antipodally symmetric distribution on the sphere,
The Annals of Statistics, vol. 2, no. 6, pp. 1201–1225, 1974.
- [9] K. V. Mardia and P. E. Jupp
Directional Statistics.
John Wiley & Sons, 2000.
- [10] G. Kurz, I. Gilitschenski, S. Julier, and U. D. Hanebeck
Recursive Bingham filter for directional estimation involving 180 degree symmetry,
Journal of Advances in Information Fusion, vol. 9, no. 2, pp. 90–105, December 2014.
- [11] J. Glover and L. P. Kaelbling
Tracking the spin on a ping pong ball with the quaternion Bingham filter,
in *IEEE International Conference on Robotics and Automation*, 2014.
- [12] I. Gilitschenski, G. Kurz, S. J. Julier, and U. D. Hanebeck
Unscented orientation estimation based on the Bingham distribution,
IEEE Transactions on Automatic Control, vol. 61, no. 1, pp. 172–177, January 2016.
- [13] ———
A new probability distribution for simultaneous representation of uncertain position and orientation,
in *17th Annual International Conference on Information Fusion*, 2014.
- [14] G. Kurz, I. Gilitschenski, and U. D. Hanebeck
The partially wrapped normal distribution for SE(2) estimation,
in *IEEE International Conference on Multisensor Fusion and Information Integration*, 2014.
- [15] E. A. Wan and R. van der Merwe
The unscented Kalman filter for nonlinear estimation,
in *IEEE Adaptive Systems for Signal Processing, Communications, and Control Symposium*, 2000, pp. 153–158.

- [16] S. J. Julier and J. K. Uhlmann
Unscented filtering and nonlinear estimation,
Proceedings of the IEEE, vol. 92, no. 3, pp. 401–422, March 2004.
- [17] H. M. T. Menegaz, J. Y. Ishihara, G. A. Borges, and A. N. Vargas
A systematization of the unscented Kalman filter theory,
IEEE Transactions on Automatic Control, vol. 60, no. 10, pp. 2583–2598, 2015.
- [18] P. Koev and A. Edelman
Efficient evaluation of the hypergeometric function of a matrix argument,
Mathematics of Computation, vol. 75, no. 254, pp. 833–846, January 2006.
- [19] A. Kume and A. T. A. Wood
Saddlepoint approximations for the Bingham and Fisher-Bingham normalising constants,
Biometrika, vol. 92, no. 2, pp. 465–476, June 2005.
- [20] I. Gilitschenski, G. Kurz, S. J. Julier, and U. D. Hanebeck
Efficient Bingham filtering based on saddlepoint approximations,
in *IEEE International Conference on Multisensor Fusion and Information Integration*, 2014.
- [21] T. Sei and A. Kume
Calculating the normalising constant of the Bingham distribution on the sphere using the holonomic gradient method,
Statistics and Computing, vol. 25, no. 2, pp. 321–332, April 2013.
- [22] J. Glover
“Bingham statistics library,”
2009.
- [23] A. H. Jazwinski
Stochastic Processes and Filtering Theory.
Elsevier, 1970.
- [24] D. Mortari
On the rigid rotation concept in n-dimensional spaces,
The Journal of the Astronautical Sciences, vol. 49, no. 3, pp. 401–420, 2001.
- [25] A. J. Sinclair and J. E. Hurtado
Minimum parameter representations of N-dimensional principal rotations,
Journal of the Astronautical Sciences, vol. 53, no. 3, p. 317, June 2005.
- [26] F. Thomas and A. Pérez-Gracia
On Cayley’s factorization of 4D rotations and applications,
in *6th Conference on Applied Geometric Algebras in Computer Science and Engineering*, 2015.
- [27] K. Levenberg
A method for the solution of certain problems in least squares,
Quarterly of Applied Mathematics, vol. 2, pp. 164–168, 1944.
- [28] D. Marquardt
An algorithm for least-squares estimation of nonlinear parameters,
SIAM Journal Applied Mathematics, vol. 11, pp. 431–441, 1963.
- [29] W. H. Clohessy and R. S. Wiltshire
Terminal guidance system for satellite rendezvous,
Journal of Aerospace Science, vol. 27, no. 9, pp. 653–658, 1960.
- [30] K. T. Alfriend, S. R. Vadali, P. Gurfil, J. P. How, and L. S. Berger
Spacecraft Formation Flying.
Elsevier, 2010.
- [31] D. A. Vallado
Fundamentals of Astrodynamics and Applications.
Microcosm, 2001.
- [32] J. L. Crassidis, F. L. Markley, and Y. Cheng
Survey of nonlinear attitude estimation methods,
Journal of Guidance, Control, and Dynamics, vol. 30, no. 1, pp. 12–28, January–February 2007.
- [33] J. L. Crassidis and J. L. Junkins
Optimal Estimation of Dynamic Systems.
CRC press, 2011.
- [34] G. McLachlan and T. Krishnan
The EM Algorithm and Extensions.
John Wiley & Sons, 2008.



Jacob E. Darling is a Ph.D. candidate in Aerospace Engineering at Missouri University of Science and Technology in Rolla, MO, USA. He received his B.S. in Aerospace Engineering from Missouri University of Science and Technology in 2011. He is a Science, Mathematics, and Research for Transformation (SMART) fellow and will begin employment as a research Aerospace engineer for the United States Air Force Research Laboratory in early 2017. His research interests include dynamic pose estimation, attitude determination, spacecraft navigation, IMU-based navigation, and spacecraft relative motion.



Kyle J. DeMars is an assistant professor of Aerospace Engineering at Missouri University of Science and Technology in Rolla, MO, USA. Dr. DeMars received his Ph.D. degree in 2010, his M.S.E. degree in 2007, and his B.S. degree in 2004, all in Aerospace Engineering from The University of Texas at Austin. His research interests are in nonlinear uncertainty prediction and Bayesian inference, orbit determination, attitude dynamics and determination, data association, and autonomous sensor management.